



universität  
wien

# MASTERARBEIT

Titel der Masterarbeit

„Neuromyelitis optica like lesions in the central nervous system of experimental autoimmune encephalomyelitis rats“

verfasst von

Marko Pende, BSc

angestrebter akademischer Grad

Master of Science (MSc)

Wien, 2014

Studienkennzahl lt. Studienblatt: A 066 834

Studienrichtung lt. Studienblatt: Masterstudium Molekulare Biologie

Betreut von: o. Univ.-Prof. Dr. Hans Lassmann



# Index

1. Zusammenfassung.....	5
2. Abstract .....	7
3. Introduction.....	8
3.1 Neuromyelitis optica .....	8
3.2 Anti-AQP4 antibodies in NMO.....	9
3.3 Histology of NMO .....	10
3.4 Clinical symptoms and pathological differences of NMO and MS.....	15
3.5 Goal of work .....	22
4. Materials and Methods .....	23
4.1 Animals.....	23
4.1.1 Experimental autoimmune encephalomyelitis (EAE).....	23
4.2 Media for cell culture .....	24
4.2.1 T-cell growth factor (TCGF) Medium.....	24
4.2.2 Restimulation medium for T-cells .....	24
4.2.3 Freezing medium .....	24
4.3 Immunization of rats .....	25
4.4 Establishment of primary T-cell culture .....	25
4.5 T-cell propagation .....	26
4.6 Preparation of APCs .....	26
4.7 Antigen dependent T-cell activation (Restimulation) .....	27
4.8 Freezing of T-cells.....	28
4.9 Separation of activated lymphocytes and dead or inactive cells trough density gradient centrifugation (optional if needed).....	29
4.10 EAE induction .....	30
4.11 Tissue staining methods .....	32
4.11.1 Immunohistochemistry (IHC) .....	32
4.11.2 IHC with ABC-System (for light microscopy) .....	32
4.11.3 Double staining for fluorescence microscopy .....	35
4.11.4 Haemalaun (Haematoxylin)-Eosin staining .....	37
4.11.5 Klüver-Pas staining .....	38
4.11.6 Bielschowsky staining.....	39
4.12 Quantification.....	40
4.12.1 Semi quantitative scoring.....	40
4.12.2 Quantitative analysis .....	40
5. Results .....	41

5.1 Basic pathology of NMO-like lesions induced by NMO IgG in combination with encephalitogenic T-cell in Lewis rat model. ....	41
5.2 In the cortex of EAE rats human anti-aquaporin antibodies induce stronger microglia activation than subcuvia or T-cells alone. ....	42
5.3 Detailed description of cortical lesion pathology induced by NMO IgG in EAE rats. ....	46
5.4 AQP4 and GFAP loss is induced in EAE after transfer of selected MBP reactive T-cell lines in the absence of pathogenic antibodies. ....	48
5.5 Tissue vacuolization (spongy degeneration) precedes AQP4 and GFAP loss in T-cell mediated EAE lesions.....	50
5.6 No major histocompatibility complex (MHC) II expression on astrocytes in T-cell mediated EAE lesions. ....	54
6. Discussion .....	56
6.1 Cortical lesions .....	56
6.2 T-cell induced astrocyte damage .....	60
7. Conclusion .....	62
8. Acknowledgements .....	63
9. References.....	64

# 1. Zusammenfassung

Neuromyelitis optica (NMO) ist eine schwerwiegende Autoimmunerkrankung die durch Entzündung, den Verlust von Astrocyten und starker Demyelinisierung in den zentralen Nervensystem (ZNS) charakterisiert ist. Die Hauptangriffspunkte dieser Erkrankung sind die graue Substanz in dem Rückenmark und der optische Nerv. NMO Patienten leiden an Schmerzen, Sehstörungen, Verlust von motorischen und sensorischen Fähigkeiten als auch an Symptomen die in Zusammenhang mit dem autonomen Nervensystem assoziiert werden wie z.B. Erbrechen und Schluckauf. Es wurde für lange Zeit erachtet, dass NMO ein Subtyp von Multiple Sklerose (MS) ist, allerdings mit deutlichem klinischem, radiologischem und neuropathologischen Erscheinungsbild.

Ein diagnostischer Durchbruch für die Charakterisierung dieser Krankheit ist das Vorhandensein von dem spezifischen Autoantikörper welcher den Aquaporin-4 (AQP4) Wasserkanal als Ziel hat. Dieser anti-AQP4 Antikörper ist mit bis 98% hoch spezifisch für NMO und kommt in mehr als 75% aller NMO Patienten vor. AQP4 ist der häufigste Wasserkanal im ZNS und ist vorwiegend auf den subpialen astrocytischen Fortsätzen welche die Glia limitans formen, auf den ependymalen und subependymalen Fortsätzen und an den perivaskulären astrocytischen Endfüßen exprimiert. Es ist noch immer nicht ganz aufgeklärt was die Produktion dieser AQP4 spezifischen Antikörper einleitet, wie diese Antikörper die Blut-Hirn-Schranke passieren und welche Mechanismen genau hinter der Entstehung der Läsionen stecken. Weiterst scheint es, dass die NMO Immunglobuline (IgG) aus verschiedenen Patienten unterschiedliche Segmente des supramolekularen Komplexes von AQP4 erkennen und mit unterschiedlicher Affinität an den AQP4 Wasserkanal binden.

In dieser Arbeit habe ich die NMO IgG Seren aus acht verschiedenen Patienten in experimentellen autoimmune encephalomyelitis Ratten, auf ihr Vermögen NMO Läsionen im Rückenmark und Cortex zu erzeugen, untersucht.

Weiterst habe ich die Interaktion von dem Immune System (IS) mit den anti-AQP4 spezifischen Antikörper in NMO ähnlichen Läsion im EAE Tiermodell beschrieben. Interessanterweise fand ich heraus, dass eine der MBP T Zell Linien, welche wir für die Induktion der EAE verwendet haben, starke astrocytische Degeneration, ohne das Vorhandensein von humanem NMO IgG, verursacht.



## 2. Abstract

Neuromyelitis optica (NMO) is a severe autoimmune disease characterized by inflammation, astrocyte loss and profound demyelination in the central nerve system (CNS). The main targets are grey matter of the spinal cord and the optic nerve. Patients suffer from visual impairment, motoric and sensory loss, pain as well as symptoms caused by the affected autonomous nervous system like nausea and hiccups. For long it was believed that NMO is a subtype of multiples sclerosis (MS) with distinct clinical, radiological and neuropathological onset.

A diagnostic breakthrough of this disease was the presence of a specific autoantibody called NMO-IgG that targets the aquaporin-4 (AQP4) water channel on astrocytes. This anti-AQP4 antibody is specific for up to 98% for NMO and can be found in more than 75% of all NMO patients. AQP4 is the main water channel in the CNS and is primarily localized on the subpial astrocytic processes that form the glia limitans, the ependymal and subependymal processes and the perivascular astrocyte endfeet. It is still not completely understood what induces the production of these AQP4 specific antibodies and how these antibodies pass the blood brain barrier (BBB). The mechanisms behind the lesion formation are partially elucidated. Further, it seems that NMO immunoglobulin G (IgG) from different patients recognize different segments of the AQP4 supramolecular complex which results in differences in binding affinity for the AQP4 channel of each NMO IgG in different patients.

Here I analyzed the NMO IgG sera from eight different patients in experimental autoimmune encephalomyelitis induced in rats (EAE) and aimed to highlight their capability of inducing NMO-like lesion in the spinal cord and the cortex.

Further, I described the interaction of the immune system (IS) with the anti-AQP4 specific antibodies in NMO-like lesion. Interestingly, I also found that one of the MBP T-cell lines which we used to induce EAE causes strong astrocyte damage without the presence of human NMO IgG.

## 3. Introduction

### 3.1 Neuromyelitis optica

Neuromyelitis optica has originally been defined as an idiopathic inflammatory demyelinating disorder associated with transverse myelopathy and optic neuritis (Davis et al., 1996). NMO was considered a subtype of multiples sclerosis (MS), though with characteristic clinical, pathological and radiologic features (Lucchinetti et al., 2002; Misu et al., 2006; Ransohoff, 2012; Roemer et al., 2007; Vaknin-Dembinsky et al., 2012).

A diagnostic hallmark was the discovery of a serum autoantibody with high specificity for this disease (Lennon et al., 2004). This autoantibody can be detected in more than 75% of all NMO patients (Waters et al., 2008) and is directed against the aquaporin-4 (AQP4) water channel located mainly on the end feet of astrocytes (Jarius et al., 2008; Lennon, 2005). The high diagnostic sensitivity of this antibody as a marker allowed to define the clinical spectrum of the disease (Matiello et al., 2008; Takahashi et al., 2008; Wingerchuk et al., 2007), which differs from that seen in classical MS in essential aspects (Pittock et al., 2006; Wingerchuk et al., 2006; Wingerchuk et al., 2007).

Despite of negative brain Magnetic Resonance Imaging (MRI) was considered as a required diagnostic condition for NMO (Wingerchuk et al., 1999), findings in the last years indicate that either symptomatic or asymptomatic, MS typical and atypical brain lesions are often seen in NMO (Pittock et al., 2006; Wingerchuk et al., 2006). Former (Filippi et al., 1999; Rocca et al., 2004; Yu et al., 2006) and further MRI studies show evidence that these lesions may be one of the representing features of the disease (Asgari et al., 2011b; Kim et al., 2011a; Kim et al., 2011b; Kim et al., 2010; Saiki et al., 2009; Saji et al., 2013; Yu et al., 2008). However there are very few pathological findings in post mortem cortex tissue (Saji et al., 2013) and some studies even report no evidences of cortical lesions in NMO at all (Calabrese et al., 2012; Popescu et al., 2010).



### 3.2 Anti-AQP4 antibodies in NMO

As mentioned above the discovery of anti-AQP4 antibodies present in most of the NMO patients sera (Lennon et al., 2004) was a major breakthrough in the diagnosis of the disease but before that, evidence already pointed to an antibody-associated disease mechanism. Early neuropathological findings of the disease showed perivascular deposition of IgG and IgM and with it associated complement activation (Lucchinetti et al., 2002). The importance of the AQP4 specific antibodies is now universally accepted, but the role of these antibodies in the pathogenesis of NMO is currently debated.

On the one hand, it was observed that NMO antibody titers rise before a relapse and stay higher during the relapse in comparison to the remission state, as well suggesting that higher titers are also associated with more severe attacks (Jarius et al., 2008; Takahashi et al., 2007a). It was shown that treatment strategies like plasma exchange and B cell depletion improve the medical conditions of NMO patients (Cree et al., 2005). Additionally it was demonstrated that AQP4 specific antibodies together with activated complement can cause AQP4 loss (Saadoun et al., 2010). Further it was speculated that the anti-AQP4 antibodies can enter the CNS without inflammation or cell mediated help (Jarius and Wildemann, 2010).

On the other hand, there is strong evidence that high AQP4 antibody titers alone are not enough to induce NMO. Some case reports tell about high anti-AQP4 IgG titer years before the disease onset without any clinical signs of NMO (Nishiyama et al., 2009) or display high or unchanged antibody titer during remission (Jarius et al., 2008; Jarius et al., 2008c; Takahashi et al., 2007b). Moreover other case reports describe that mothers with NMO do not transfer the disease to their newborn babies despite the fact that AQP4 antibodies are IgG1 and easily can pass the placenta (Cornelio et al., 2009; Tsugawa et al., 2010). Previous findings from our lab showed that three weeks old rat, which still have physiologically a leaky blood brain barrier, injected with NMO IgG show no NMO pathology but if the same experiment was performed in the presence of CNS specific T-cells NMO-like lesions could be induced (Bratl et al., 2009). Additional findings report significantly elevated levels of proinflammatory cytokines in the CSF of NMO patients (Tanaka et al., 2008).

### 3.3 Histology of NMO

The classic pathological characteristics of NMO lesions span more than three spinal cord vertebral segments (Wingerchuk et al., 2006). They are associated with necrosis and severe axon pathology in gray and white matter (Figure 1 A and 2C) and with pronounced loss of oligodendrocytes (ODC) in the lesion (Figure 2D).

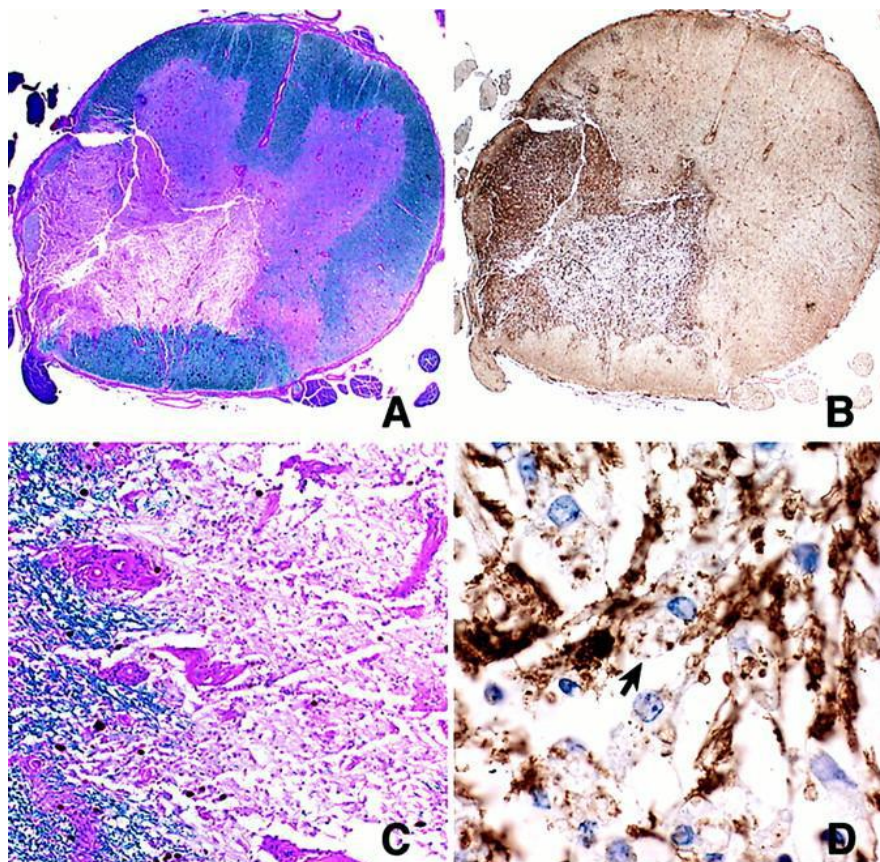


**Figure 1** Histopathology of NMO. (A) Staining of the spinal cord cross-section with Luxol fast blue and PAS myelin stain demonstrates major demyelination affecting both grey and white matter (10x magnification). (B) The lesion is formed by numerous macrophages, which have been stained using KiM1P pan-macrophage stain (10x magnification). (C) One can distinguish very nicely between the periplaque white matter and the plaque after Luxol fast blue and PAS myelin stain (100x magnification). (D) As pointed out by the arrow macrophages contain myelin debris within their cytoplasm (MOG-Immunocytochemistry, 600x magnification). Picture and legend are taken from (Lucchinetti et al., 2002)

The inflammatory infiltrates of NMO lesions consist mainly of macrophages/microglia (Figure 1B and 4G, E) and granulocytes (Figure 3 A and B), B-cells and few CD3+ and CD8+ T-cells (Figure 2 A and B).

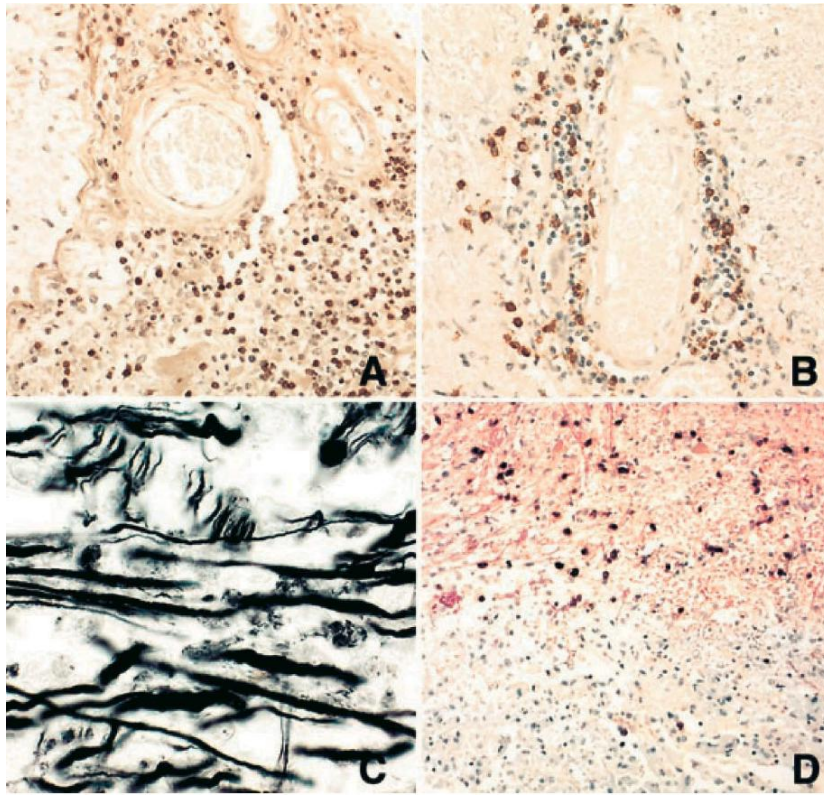


**Figure 2** Histopathology of neuromyelitis optica. (A, B, mag 3200) The perivascular infiltrate contains numerous CD3+ T lymphocytes (A) and CD8+ T lymphocytes (B). (C). There is a marked reduction in axonal density and acute axonal pathology consisting of swellings and spheroids (Bielschowsky silver impregnation, mag 3400). (D) There is a marked reduction in oligodendrocytes within the lesion [PLP mRNA in situ hybridization (black); double-labelled with immunocytochemistry for PLP protein (red, mag 3200)]. Picture and legend are taken from (Lucchinetti et al., 2002)

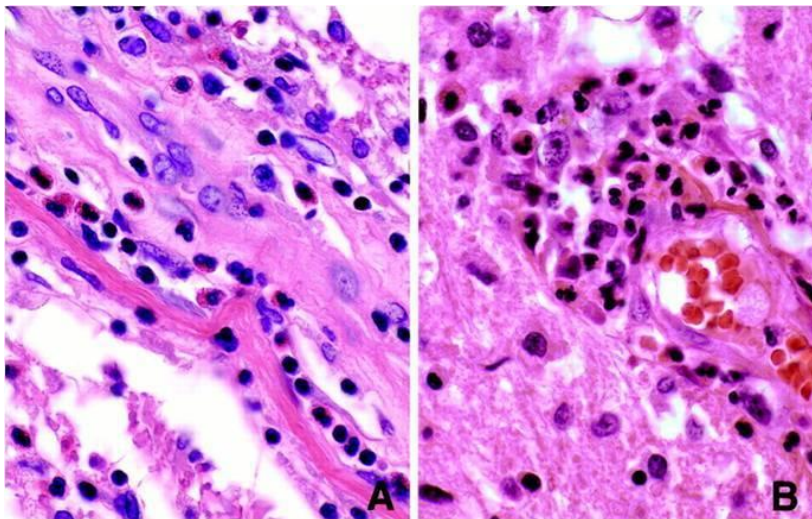


**Figure 3** Inflammatory infiltrate in NMO. Numerous perivascular eosinophils (A) and granulocytes (B) are located within the lesion (haematoxylin–eosin, mag ×600). Intact perivascular and parenchymal eosinophils are present within the lesion (haematoxylin–eosin, mag ×100) Picture and legend are taken from (Lucchinetti et al., 2002)

AQP4 is mainly located at astrocyte endfeet surrounding perivascular regions in the CNS (Jarius et al., 2008; Lennon, 2005). Deposition of Ig and the C9 complement subunit can be found at this site (Figure 4 B,C,D and E) and are accompanied by AQP4 loss and astrocyte degeneration (Bradl et al., 2009).



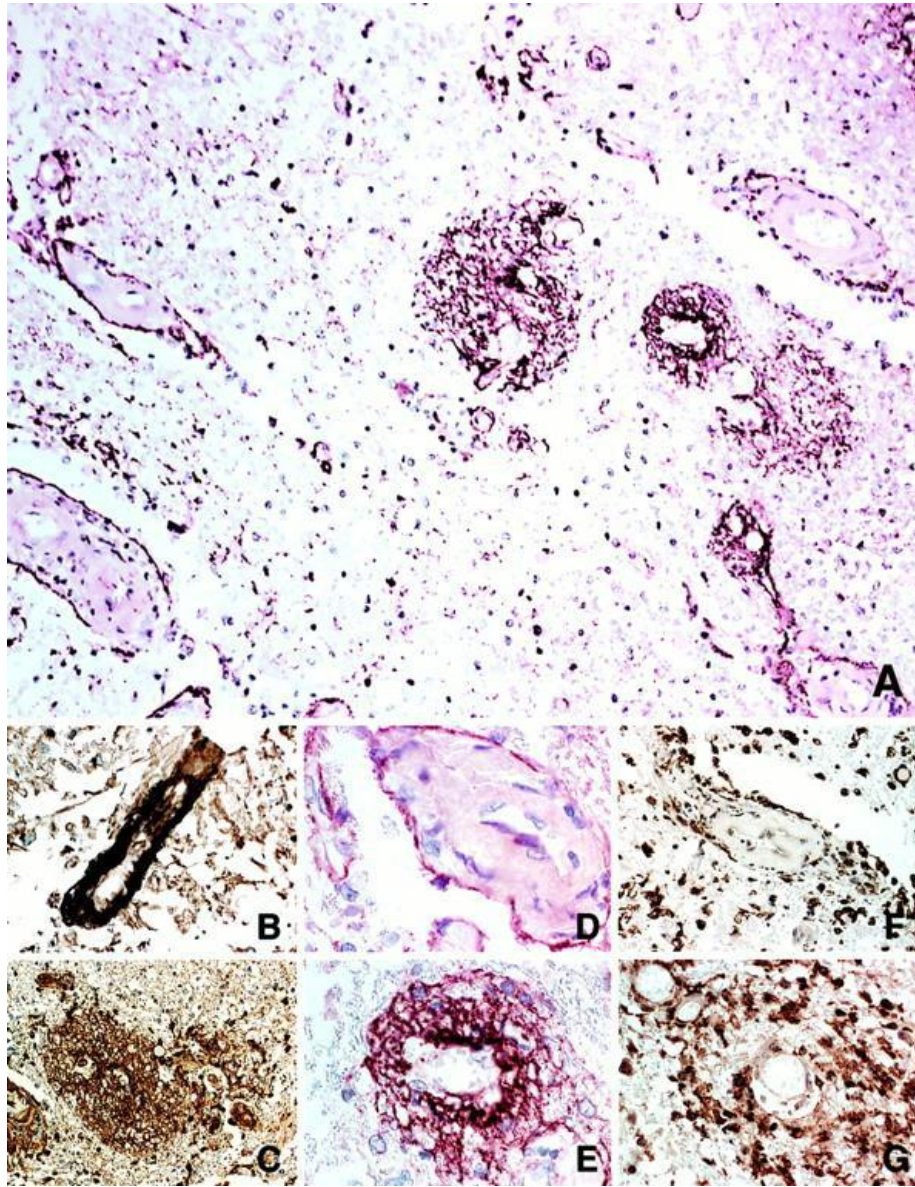


**Figure 4** One can see the participation and deposition of complement components in active demyelinating lesions of NMO patients. (A) An active lesion showing deposition of C9neo-antigen (red staining) on the outer surface of thickened blood vessels, as well as in a rosette-like pattern (200x magnification). (B) The immunoglobulin reactivity (human Ig) is pronounced in the perivascular space. (C) Immunocytochemistry for IgM demonstrates a rosette perivascular staining pattern. Higher power view of staining for complement activation with C9neo-antigen (red) demonstrates this rim (D) and rosette (E) pattern of staining. Macrophages co-localize in a similar rim (F) and rosette (G) pattern (KiM1P pan-macrophage stain) (mag ×400). Picture and legend are taken from (Lucchinetti et al., 2002)

Chronic NMO lesions are characterized by astrocytic gliosis, atrophy, cavitation (Asgari et al., 2011b; Bradl et al., 2009; Jarius et al., 2008; Lucchinetti et al., 2002; Roemer et al., 2007) and increase in numbers and prominence of thickened hyalinized blood vessels within the lesion.

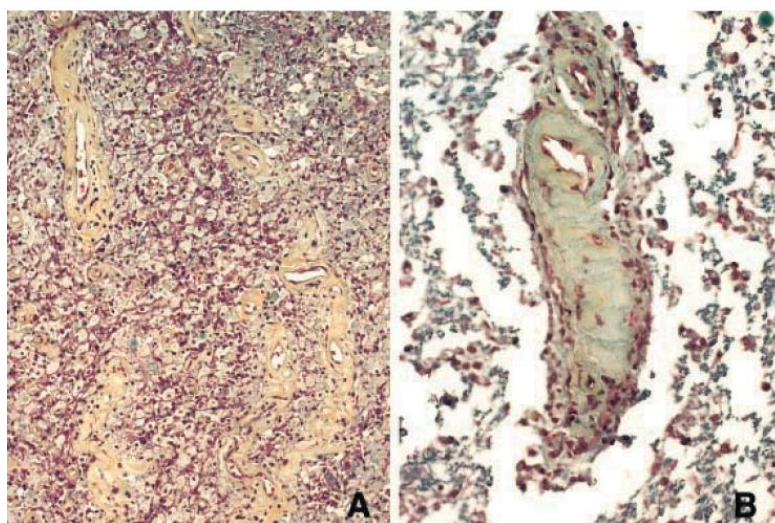


**Figure 5** Vessel pathology in NMO. (A) There is an apparent increase in numbers and prominence of thickened hyalinized blood vessels within the lesion (Movat, mag 3100). (B) Higher power view emphasizes collagen infiltration of vessel wall (green with Movat, mag 3400). Picture and legend are taken from (Lucchinetti et al., 2002)

New pathological findings suggest at least six different lesion types in NMO (Table 1) (Misu et al., 2013). The pathology describe above would be classified as a lesion Type I. Further lesion types are described as followed.

In type II lesions most cellular components are lost and replaced by fluid filled cysts, which contain a variable number of macrophages, disintegrated astrocytes and vessels with perivascular fibrosis. In several areas some bipolar and unipolar GFAP-positive progenitor cells can be observed (Parratt and Prineas, 2010). Lesion type III was present in white matter tracts of spinal cord. These lesions show signs of secondary Wallerian degeneration with extensive loss of myelin, axons and ODC together with severe fibrillary gliosis characterized by densely packed GFAP and AQP1 reactive astrocyte processes. The loss of AQP4 is variable. Lesion type IV displays strong AQP4 loss with no complement activation or granulocytes, variable degree of macrophages and complete preservation of GFAP and AQP1 signal. Type V are white matter lesions with inflammatory infiltrates consisting of T-cells and macrophage infiltration and extensive astrocyte apoptosis in the absence of complement deposition. Astrocytes show very few surface AQP1 and AQP4 but display intracellular granules reactive for these proteins. Additionally, no axonal injury or demyelination can be monitored in this lesion type. The sixth lesion type is characterized by astrocyte dystrophy and primary demyelination, reflected by macrophages with early myelin degradation products. Additionally, inflammatory T-cell infiltrates are present.

**Table 1** Key pathological features of different lesions types in NMO. Table was taken from (Misu et al., 2013)

Les. Type	T	Gr	C9n	AG	Demy	OG loss	Ax loss
1	++	+++	+++	Necrosis AQP4 variable AQP1 variable GFAP variable	+	Apo	+
2	+ / +++	±	±	AQP4 loss AQP1 loss GFAP loss	Complete	+++	+++
3	-	-	-	React. gliosis	+++	++	+++
4	±	-	-	AQP4 loss Clasmatodendrosis +	-	-	-
5	++	-	-	Clasmatodendrosis +++ AQP4 loss AQP1 loss GFAP loss	-	-	-
6	++	-	-	Clasmatodendrosis + / +++ AQP4 loss variable AQP1 loss variable GFAP loss ±	Complete	+++	++

Les.Type lesion type, T T-cells, Gr granulocytes, C9n complement C9neo antigen, AG astroglia pathology, Demy demyelination, OG loss loss of oligodendrocytes, Ax. Loss axonal loss ±, minor or absent; +, minor; ++, moderate; +++, severe

Interestingly, in a study with 43 EAE rats, treated with different NMO-IgG sera (n20) and controls (Subcuvia=n13, PBS=n10), I could observe a further lesion type with profound, patchy AQP4 and GFAP loss and preserved myelin, in the presence and absence of AQP4 specific antibodies.

It was already described that NMO-like lesions in animal models can be induced by injection of lipopolysaccharide (LPS) in the absence of AQP4 specific antibodies which leads to initial microglia activation and is followed by retraction of astrocytic foot processes at the glia limitans and loss of AQP4 (Sharma et al., 2010). Other data suggests that CD4<sup>+</sup> T-cells can induce tissue injury also in an antigen independent way (Nitsch et al., 2004).

Traditionally, the only function of astrocytes considered was to provide nutrition support as well as protection for the neuron and to produce a glia scar in CNS lesions. However, it has become increasingly clear that astrocytes are also key player in the regulation of immune response within the spinal cord and brain. They express diverse receptors related to innate immunity such mannose receptors, scavenger receptors, toll-like receptors (TLRs), nucleotide binding oligomerization domains and dsRNA dependent protein kinases (Farina et al., 2007). Activated astrocytes produce complement associated components and immunomodulatory and immunopathogenic cytokines e.g. interleukin 1 (IL-1), IL-6, IL-10, IL-33 and tumor necrosis factor alpha (TNF-α) and chemokines e.g. monocyte chemotactic protein 1 (MCP-1), IL-8, CCL-5 and interferon gamma induced protein 10

(IP-10) (Carpentier et al., 2005; Chakraborty et al., 2010; Oh et al., 1999). Some in vitro studies also suggest that astrocytes are capable of MHC II expression (E Ulvestad, 1994; Fierz et al., 1985; Fontana et al., 1984). Another study suggest that IL-1 $\beta$  release and the following production and accumulation of complement factors e.g. C1q facilitates neutrophil entry and BBB breakdown in the proximity of NMO lesions and might thus be important secondary factors for lesion formation (Kitic et al., 2013).

All these findings taken together propose that under conditions of severe inflammation lesion formation with astrocyte injury may occur even in the absence of astrocyte targeting antibodies, such those present in NMO IgG.

### **3.4 Clinical symptoms and pathological differences of NMO and MS**

The median age of NMO onset is 39 years which is ten years later than in MS (Wingerchuk et al., 1999) and occurrence of the disease varies in different ethnic groups. In Europe, Australia and North America only 1-2% suffering from a demyelinating disease are diagnosed with NMO whereas about 5% of African-American, 23% of the Brazilian, more than 30% of Asians and 90% of Black-Africans do so (Jarius et al., 2008c; Wingerchuk et al., 2007).

NMO can be divided into three clinical courses. In 10% of the NMO cases simultaneous bilateral optic neuritis and transverse myelitis can be seen. This is termed the classical Devic's syndrome. In 2% of the patients the disease occurs with progression. These patients have a very poor prognosis and frequently develop respiratory failure during attacks of cervical myelitis. The most common form of NMO (80-90%) is a relapsing remitting course where transverse myelitis and optic neuritis is more often occur separately than simultaneously and the intervals between the attacks can last from years to decades (Jarius et al., 2008; Misu et al., 2005). Interestingly, the relapsing-remitting NMO disease pattern is more frequent in woman than in men (Nandhagopal et al., 2010) and the risk of having a relapse is increased post partum in comparison to other patients (Bourre et al., 2012; Cornelio et al., 2009; Tsugawa et al., 2010).

NMO is characterized by acute optic neuritis and longitudinally extensive severe myelitis (Wingerchuk et al., 1999) (Figure 8). Therefore, NMO patients mostly suffer from visual interference, often simultaneously with periocular pain due to eye movement, up to complete blindness. They often have muscle weakness in all four limbs up to paralysis of the lower limbs (Sato and Fujihara, 2011). The accumulation of irreversible deficits and the fast progression of the



disease lead to a mortality rate of about 30% in the first five years in patient with a relapsing remitting course (Wingerchuk et al., 1999).

As already mentioned NMO has been considered as a subtype of MS for a long time, although with distinct radiological, clinical and neuropathological findings (Jarius et al., 2008c; Wingerchuk et al., 2006). After the discovery of the potential of AQP4 antibodies as a marker for NMO and the redefinition of diagnostic MRI criteria, it became possible to distinguish between these two diseases. MS is in contrast to NMO a chronic inflammatory primary demyelinating disease of the CNS and is associated with reactive glial scar formation and profound myelin loss, while the axons remain relatively well preserved in relation to the demyelination (Lassmann, 2005). NMO lesions are predominantly found in the grey matter (Nakamura et al., 2008) with granulocytic infiltrates and vascular associated IgG, IgM deposition and complement activation (Jarius et al., 2008d; Lucchinetti et al., 2002; Wingerchuk et al., 2007a) while MS lesions can be found in white matter with inflammatory infiltrates consisting of T-cells, B-cells (Esiri, 1980; Esiri et al., 1989) and spatially associated complement to activated microglia/macrophages and oligodendrocytes at the lesion edge (Jarius et al., 2008; Lucchinetti et al., 2002; Traugott et al., 1983), (Table 2) (Figure 6).

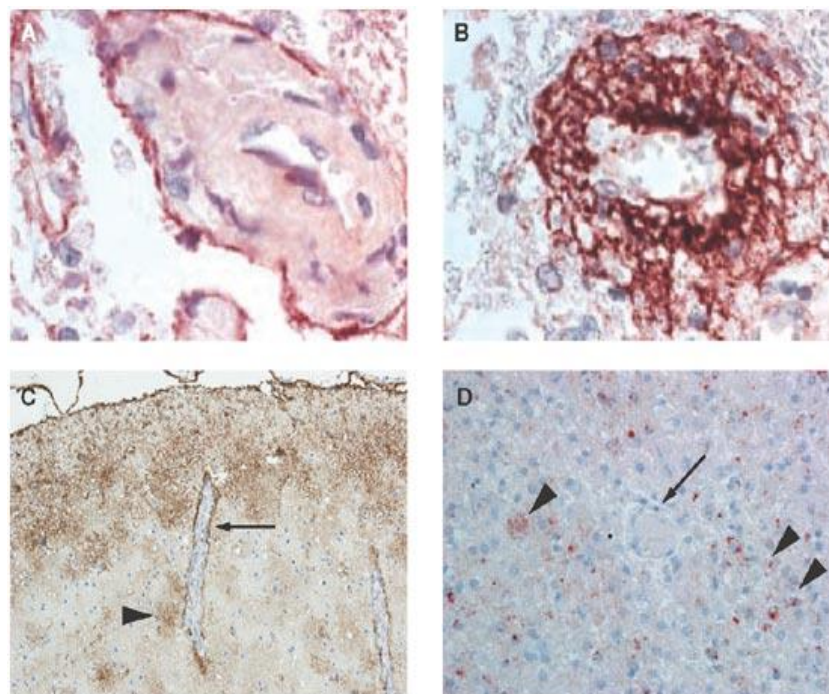


**Figure 6** Complement deposits at sites of AQP4 loss in neuromyelitis optica but not in multiple sclerosis. Neuromyelitis optica lesions are characterized by (A) a distinct perivascular rim or (B) a rosette or mesh pattern of complement C9neo deposition, which corresponds well to (C) perivascular AQP4 (brown) expression in the healthy CNS. (D) By contrast, in type II multiple sclerosis lesions, complement deposits (C9neo, brown) are found within macrophages (arrow heads) and on oligodendrocytes at the lesion edge (not shown), but not around vessels (arrow). Pictures are taken from (Jarius et al., 2008)



**Table 2** Comparison of MS and NMO. Table was taken from (Jarius et al., 2008)

Neuromyelitis optica	Multiple sclerosis
White and gray matter involvement	Predominant white matter involvement
Striking edema	Inflammatory lesion
Necrosis	Necrosis not striking
Cavitations	No cavitations
Relatively preserved myelin in some lesions	Severe demyelination
Axonal damage	Axonal damage
Leukocyte infiltrates are mainly neutrophils and eosinophils rather than T and B lymphocytes	Leukocyte infiltrates are mainly T and B lymphocytes rather than neutrophils
Loss of aquaporin-4 in all lesions	Upregulation of aquaporin-4 in active lesions
Loss of glial fibrillary acidic protein in most lesions	Increased glial fibrillary acidic protein staining
Complement and IgM-IgG deposits around blood vessels	Less-marked complement deposits within macrophages and at the lesion edge on oligodendrocytes/myelin (in type II multiple sclerosis lesions)
Vascularity increased	Increased vascularity uncommon

In NMO AQP4 and GFAP loss are one of the main characteristic features of the disease and are stage independent, whereas in MS there is either upregulation of AQP4 in the rim of active or remyelinating lesions or loss in chronic lesions (Misu et al., 2007; Misu et al., 2006; Pittock et al., 2006; Roemer et al., 2007) (Figure 7).

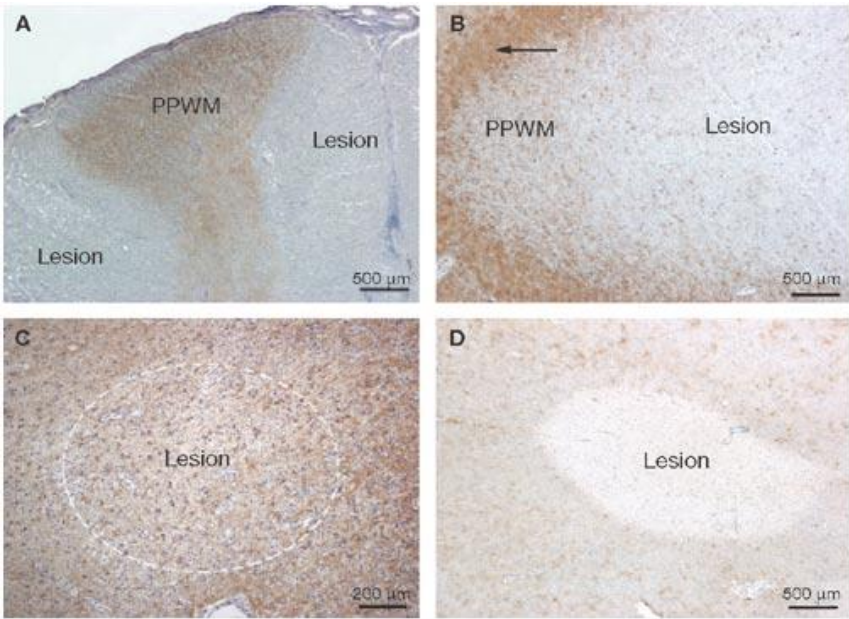


**Figure 7** AQP4 expression in neuromyelitis optica and multiple sclerosis. All images show spinal cord lesions. (A) In neuromyelitis optica, a marked and stage-independent loss of AQP4 (brown) is found within spinal cord lesions, although it is retained in the periplaque white matter. (B,C,D) AQP4 immunoreactivity (brown) is stagedependent in multiple sclerosis. In the case of active demyelinating lesions (B), AQP4 expression is increased in the adjacent cortical gray matter (arrow) and periplaque white matter. In active remyelinating lesions (C), there is diffusely increased expression in both the center of the lesion and the periplaque region. In chronic inactive lesions (D), there is complete loss of AQP4. Picture and legend are taken from (Jarius et al., 2008)

Additionally, it was discovered that the cytokine levels of IL-2, IL-4, IL-10, IL-17 and IFN $\gamma$  were elevated in sera from NMO patients compared to those in MS patients. Especially an IL-2 value of

more than 5pg/mL can be used as a marker to distinguish between NMO and MS (Wang et al., 2013). Another biomarker can be the level of cerebrospinal fluid (CSF)-GFAP. It was reported that, regardless the localization of the NMO lesion, the CSF-GFAP levels during acute stages of NMO were significantly higher than those in MS (Fujihara et al., 2012; Petzold et al., 2011).

Another, although much debated, point in distinguishing NMO from MS is the presence of brain lesions in NMO. One of the first diagnostic criteria for NMO was that the absence of evidence for clinical disease outside of the optic nerve or the spinal cord (Wingerchuk et al., 1999). After the discovery of the NMO IgG these criteria were revised by Wingerchuk and new diagnostic criteria were established according to Table 3, although the criteria for the optico-spinal-lesions were not considered as crucial symptoms anymore.

**Table 3** *Proposed diagnostic criteria for NMO. Table was taken from (Wingerchuk et al., 2006)*

Definite NMO
Optic neuritis
Acute myelitis
At least two of three supportive criteria
1. Contiguous spinal cord MRI lesion extending over $\geq 3$ vertebral segments
2. Brain MRI not meeting diagnostic criteria for multiple sclerosis
3. NMO-IgG seropositive status

New MRI findings show that more than 60% of anti-AQP4 sero positive patients also display NMO specific brain lesions in areas with high AQP4 expression (Figure 8) (Asgari et al., 2011b; Kim et al., 2011; Li et al., 2008; Pittock et al., 2006; Saji et al., 2013). Such lesions can be found in e.g. the area postrema (AP) and the hypothalamus, as well as cerebro cortical lesions, which are either similar to MS lesions or are nonspecific. The comparison of cortical lesions with those found in the spinal cord or in the optic nerve show similarities with respect to type of inflammation, complement and Ig deposition and AQP4 loss. These findings indicate that cortical and already described opticospinal NMO lesions have a shared pathogenesis.

NMO lesions in the AP can induce intractable, but reversible nausea associated with persistent hiccups, vomiting or respiratory failure (Kobayashi et al., 2009; Misu et al., 2005; Nandhagopal et al., 2010; Popescu et al., 2011; Suzuki et al., 2010; Takahashi et al., 2008). In some cases hiccups and vomiting can even be initial symptoms of NMO (Apiwattanakul et al., 2010; Misu et al., 2005).

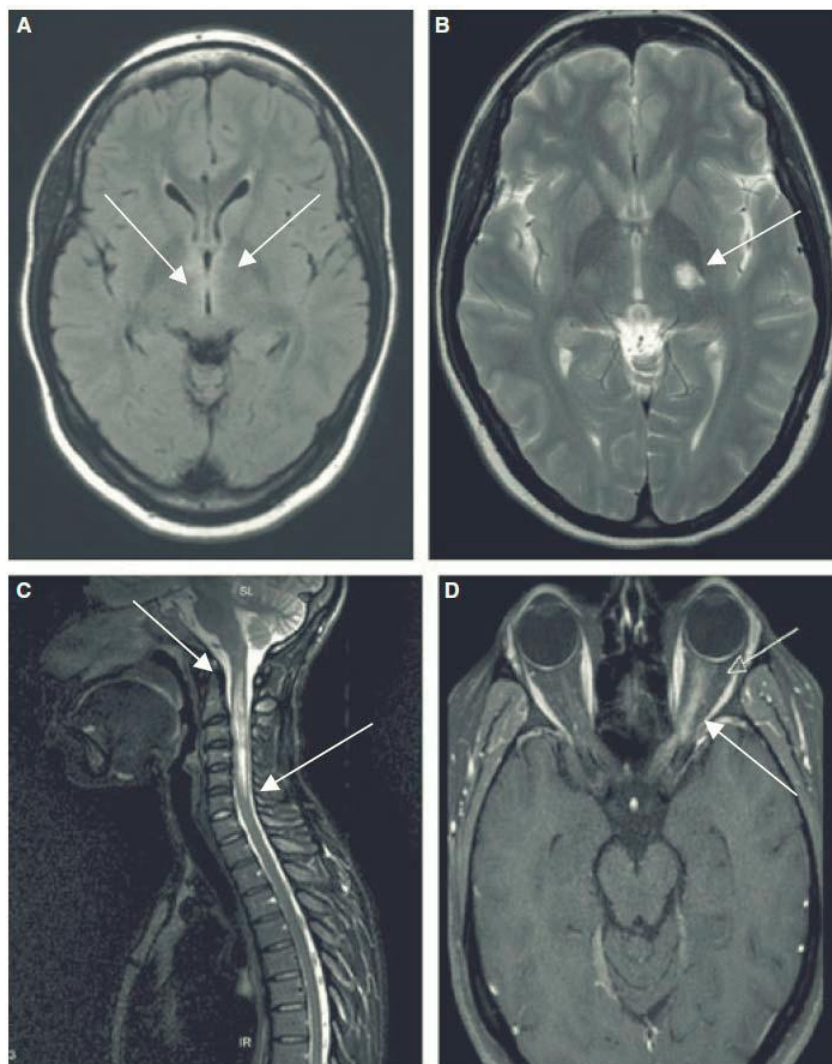


**Figure 8** Central nervous system lesions typical of neuromyelitis optica (NMO). Representative magnetic resonance imaging (MRI) of patients with NMO seropositive for anti-AQP4 antibody (NMO-IgG), from the authors (Asgari) clinic. (A) Fluid-attenuated inversion recovery (FLAIR) shows signal abnormality around the third ventricle. (B) T2-weighted MRI signal abnormality in the thalamus and posterior limb of internal capsule on the left side. (C) Sagittal T2-weighted MRI of cervical spinal cord from a patient with NMO, showing longitudinally extensive transverse myelitis with swelling. (D) Gadolinium enhancement T1-weighted image shows optic neuritis on the left side. Picture and legend are taken from (Asgari et al., 2011)

Like other circumventricular organs, the AP lacks tight junctions between the endothelial cells which makes the BBB permeable to a certain extent in this part of the CNS. Additionally, the medullary floor of the fourth ventricle and the AP are both sites with high AQP4 expression and thus indeed, inflammatory, non necrotic, non demyelinating, lesions were observed in these areas (Roemer et al.,

2007). Immunopathological investigation of neuropathology in the circumventricular organs in fifteen NMO cases revealed that six of these cases display in the AP and the medullary floor of the fourth ventricular lesions (Popescu et al., 2011). These lesions were characterized by thinning of the tissue, blood vessel thickening and general axonal and myelin preservation. Further, all six cases showed loss of AQP4, variable infiltration of inflammatory lymphocytes, prominent microglia activation and in three cases, eosinophils. Perivascular complement deposition on astrocytes and macrophages were also present in some cases.

Another area with high AQP4 expression is the cerebral cortex and indeed cortical gray matter abnormalities have been reported on MRI (Filippi et al., 1999; Pittock et al., 2006; Rocca et al., 2004; Yu et al., 2008; Yu et al., 2006). NMO cortical lesions are characterized by apoptotic neurons and pronounced gliosis, mostly involving interlaminar astroglia (Popescu et al., 2010). Activated astrocytes with prominent nuclei, clear cytoplasm and multiple, elongated and abundant thin processes were present in all cortical layers. Complement activation could not be observed in these cases. A recent study indicates that AQP4 and GFAP signal is lost in cortical layer I, but preserved on reactive astrocytes in cortical layer II to IV (Figure 9). A profound microglia reaction was also seen in cortical layer II and significant loss of neurons was observed in cortical layer II to IV (Saji et al., 2013).

These findings are in contrast to other studies that could not find brain abnormalities in NMO patients with MRI or lesions in immunohistochemically examined NMO tissue.

There are still very few reports on the pathology of brain lesion in NMO and it is hypothesized that in contrast to MS, NMO brain lesions may be reversible, if this is true it would make the detection and characterization even more difficult.



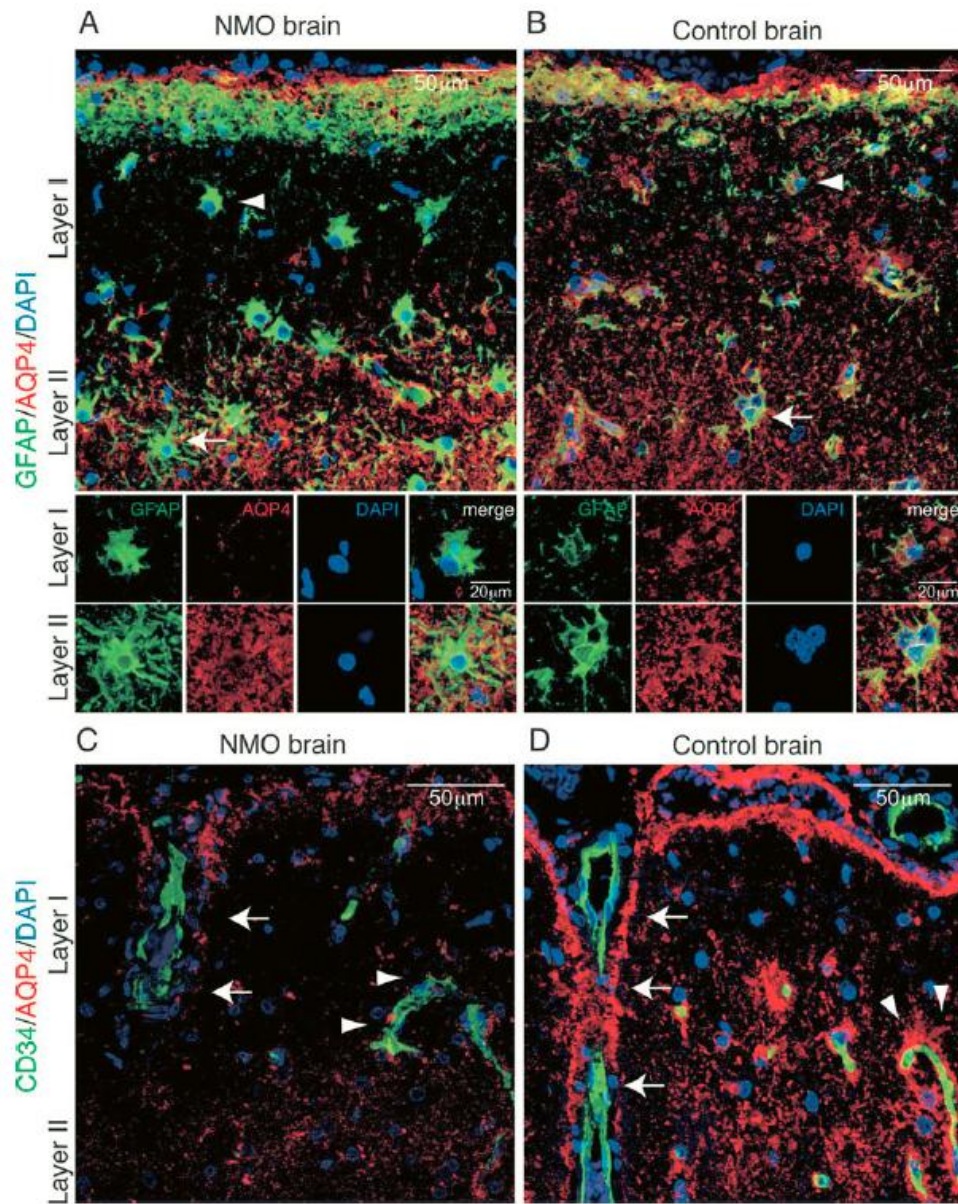


**Figure 9** Double immunofluorescence demonstrating localization of aquaporin-4 (AQP4) and either glial fibrillary acidic protein (GFAP) or CD34 in neuromyelitis optica (NMO) spectrum disorder (NMOsd) and control brains. In cortical layer I of NMOsd brains, loss of AQP4 (red) in GFAP-labeled (green) astrocytes (eg, an astrocyte indicated by an arrowhead in upper panel of A) is evident, whereas AQP4 in GFAP-labeled astrocytes in cortical layer II in NMOsd brains (an example is indicated by an arrow in the upper panel of A) and in cortical layers I and II in control brains (examples are indicated by an arrow and an arrowhead in upper panel of B) is preserved. In cortical layer I of NMOsd brains, loss of AQP4 (red) is evident in astrocyte processes consisting of glia limitans covering the Virchow–Robin spaces (arrows in C) and in astrocyte endfeet facing CD34-labeled endothelial cells (green) of cortical blood vessels (an example is indicated by arrowheads in C), whereas AQP4 (red) of glia limitans and endfeet (arrows and arrowheads in D, respectively) in cortical layers I and II of control brains are preserved. These data consistently indicated the loss of AQP4 immunoreactivity in most astrocytes in cortical layer I in NMOsd brains. Nuclei were stained blue with 4,6-diamidino-2-phenylindole (DAPI). Supplementary Figure 3 shows the preservation of AQP4 immunoreactivity in cortical layers I and II in multiple sclerosis brains, in contrast to cortical layer I in NMOsd brains. Picture and legend are taken from (Saji et al., 2013)

### **3.5 Goal of work**

As described in the introduction the presence of cortical lesions and their structural features in NMO are still highly controversial and little is known about the mechanisms of their formation. In the first part of our study we, thus, concentrated on the question, whether cortical lesions can be induced in experimental NMO models and, if this is the case to analyze their immunopathology and define the underlying mechanisms of their formation. In the second part of our study we analyzed in detail inflammatory brain lesions with astrocyte pathology, that occurred in the absence of antibodies directed against targets, expressed on the surface of astrocytes. The understanding of these lesions is important, since they occur in some instances in the multiple sclerosis brain, and their distinction from NMO lesions is important for diagnostic purposes and for the understanding of the underlying disease mechanisms.

.

## 4. Materials and Methods

All EAEs, cell cultures and serum injections were performed either by Monika Bradl, Maja Kitic or Maria Pohl.

### 4.1 Animals

Wild-type Lewis rats were bred in the decentralized facilities of the Institute for Biomedical Research (Medical University Vienna) and were sacrificed at the age of six to eight weeks. They shared cages and were housed under standardized pathogen-free conditions in a twelve hour night and day cycle.

The experiments were approved by the Ethics Committee of the Medical University Vienna and performed with the license of the Austrian Ministry for Science and Research.

#### 4.1.1 Experimental autoimmune encephalomyelitis (EAE)

EAE is an animal model and can be induced either by active immunization with CNS specific antigens (Linington et al., 1993; Mokhtarian et al., 1984; Morris-Downes et al., 2002) in complete Freund's adjuvans or passively (Linington et al., 1988; Mokhtarian et al., 1984) by the transfer of activated CNS specific T-cells (Figure 10). Active EAE leads to activation and proliferation of CNS specific T-cells and takes around twelve days until the animals develop first clinical symptoms. In passive EAE the first clinical symptoms are displayed after three to four days (Table 7).

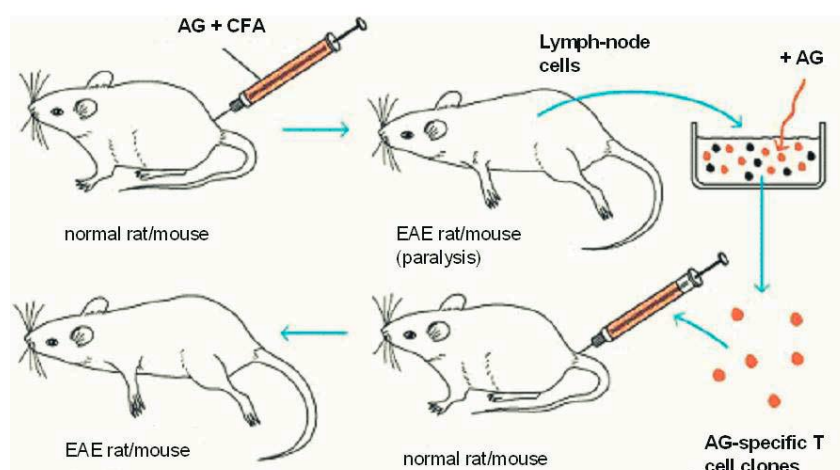


**Figure 10** Active (injection of a CNS antigen in CFA) and passive (transfer of encephalitogenic, activated T-cells) induction of EAE in animal models

## 4.2 Media for cell culture

### 4.2.1 T-cell growth factor (TCGF) Medium

- 1% (v/v) MEM non-essential amino acids (100x stock, Gibco Invitrogen, 21430-020)
- 1% (v/v) L-glutamine (200mM in 0,85% NaCl stock, Lonza, BE17-605E)
- 1% (v/v) Penicillin/Streptomycin (10000 U/ml Pen and 10000U/ml Strep, Lonza, BE17-602E)
- 1% (v/v) Na-Pyruvat (100mM stock, Gibco Invitrogen, 11360-039)
- 0,3%  $\beta$ -Mercaptoethanol ( $\beta$ -MeEtOH) (50mM stock, Sigma, M7522)
- 10% FBS (fetal bovine or calf serum, Lonza, DE14-802F)
- 10% IL-2 from MLA-IL-2-cell supernatant (own stock)

Added in Rosewell Park Memorial Institute – 1640 (RPMI-1640) (5% of CO<sub>2</sub>, Lonza, BE12-167F)

### 4.2.2 Restimulation medium for T-cells

- 1% (v/v) MEM non-essential amino acids (100x stock, Gibco Invitrogen, 21430-020)
- 1% (v/v) L-glutamine (200mM in 0,85% NaCl stock, Lonza, BE17-605E)
- 1% (v/v) Penicillin/Streptomycin (10000 U/ml Pen and 10000U/ml Strep, Lonza, BE17-602E)
- 1% (v/v) Na-Pyruvat (100mM stock, Gibco Invitrogen, 11360-039)
- 0,3%  $\beta$ -Mercaptoethanol ( $\beta$ -MeEtOH) (50mM stock, Sigma, M7522)
- 1% (v/v) rat serum (own stock)

Added in Rosewell Park Memorial Institute – 1640 (RPMI-1640) (5% of CO<sub>2</sub>, Lonza, BE12-167F)

For all media the ingredients were filtered through a sterile filter (pore size 0,22 $\mu$ m, Millipore, SCGPT02RE). The media were stored for maximum of two weeks at 4°C.

### 4.2.3 Freezing medium

- 45% RPMI-1640 (Lonza, BE12-167F)
- 45% FCS (Biochrom S01115)
- 10% DMSO (Merck, ME328)



## 4.3 Immunization of rats

### Materials

- MBP (Sigma Aldrich, M2295)
- 0.2M Sørensenbuffer (pH 7.4)
  - 40mM NaH<sub>2</sub>PO<sub>4</sub> (Merck, 1.06346.0500)
  - 160mM Na<sub>2</sub>HPO<sub>4</sub> (Merck, 1.06580.1000)
- 1 X PBS
  - 150mM NaCl (Merck, 1.06404)
  - 250ml Sørensenbuffer
  - 750ml ddH<sub>2</sub>O
- Freund's Adjuvans
  - 4 mg/ml H<sub>37</sub>Ra M. tuberculosis (Difco Laboratories, 231141)
  - Mannide Monooleate (1.5mL), Paraffin oil (8.5mL) (Difco Laboratories, 263910)

### Methods

Lewis rats were anesthetized with Isofluran and subcutaneously injected with an emulsion of 100µg of myelin basic protein (MBP) in 100µl of Phosphate buffered saline (PBS) and incomplete Freund's Adjuvant supplemented with 4 mg/ml H<sub>37</sub>Ra M. tuberculosis

## 4.4 Establishment of primary T-cell culture

### Materials

- RPMI-1640 (Lonza, BE12-167F)
- Mesh (100µm mesh size, Becton Dickinson, 352360)
- MBP (Sigma Aldrich, M2295)
- Restimulation medium ( own stock, see 4.2.2)

### Methods

The rats were sacrificed nine to twelve days after immunization by using CO<sub>2</sub>. At this time point high levels of activated MBP specific T-cells were in the paraaortal lymph nodes at the lumbal bifurcation of the aorta. These lymph nodes were isolated and placed in a dish containing RPMI-

1640. Then they were grinded through a mesh, centrifuged at 1300rpm, 4°C and the pellet was taken up in 5ml of restimulation medium per Ø 60mm Petri dish. 25µl of MBP (stock 2mg/ml) was added to these Petri dishes and they were incubated (37°C, 5% CO<sub>2</sub>) to activate the antigen presenting cells (APCs) and the MBP-specific-T-cells and to drive proliferation.

## 4.5 T-cell propagation

### Materials

- TCGF medium (see 4.2.1)
- Primary MBP-specific-T-cells (see 4.4)

### Methods

After one to three days the cells from the primary culture increase in size and form clusters (Figure 10). At this time point the IL-2 receptors on the MBP-specific-T-cells are up regulated and the cells proliferate in response to exogenous IL-2. Therefore, the cells were centrifuged and the pellet was resuspended in 10ml of T-cell growth factor (TCGF) medium and transferred in Ø 100mm dishes. The cells were incubated (37°C, 5% CO<sub>2</sub>) until their IL-2 driven proliferation does not respond any more to IL-2 treatment and they stop to form clusters and become smaller. To restart the proliferation the MBP-specific-T-cells had to be restimulated with their specific antigen in presence of freshly prepared APCs (see 4.6)

## 4.6 Preparation of APCs

### Materials

- RPMI-1640 (Lonza, BE12-167F)
- Mesh (100µm mesh size, Becton Dickinson, 352360)
- Restimulation medium (own stock, see 4.2.2)

### Methods

Animals were killed by CO<sub>2</sub> asphyxiation; the thymus was removed from them and placed sterile in a Ø 100mm dish with RPMI-1640. After dissection of the thymus through a mesh the cell

suspension was irradiated with 3000 rad (30Gy). This is to avoid the overgrowth of the MBP-specific-T-cells by the thymic cells, while the APCs maintain their ability of processing and presenting the antigen at least for the next three days. After the irradiation the cell suspension was centrifuged (1300rpm, 4°C for 10 min) and the pellet was resuspended in 10ml of restimulation medium.

## 4.7 Antigen dependent T-cell activation (Restimulation)

### Materials

- Restimulation medium (see 4.2.2)
- MBP-specific-T-cells (own stock, see 4.5)
- APCs (own stock, see 4.6)
- MBP (Sigma Aldrich, M2295)

### Methods

At the end of IL-2 driven proliferation the MBP-specific-T-cells were harvested and centrifuged (1300rpm, 4°C, for 10min) to get rid of the TCGF medium and were resuspended in restimulation medium. The cells were counted and adjusted to  $1-1,5 \times 10^6$  cells/ml.

Afterwards 3ml of restimulation medium, 1ml of MBP-specific-T-cells (containing  $1-1,5 \times 10^6$  cells), 1ml of thymic APCs (containing  $1-1,5 \times 10^8$  cells) and 25µl of MBP antigen (stock 2mg/ml) were combined per Ø60mm Petri dish and incubated (37°C, 5% CO<sub>2</sub>). After one to three days the MBP-specific-T-cells increase in size and form cluster. At this point they are prepared to be used either for further proliferation to maintain the long term cultures of MBP-specific-T-cells (see 4.5, 4.6, 4.7), to T-cell transfer into Lewis rats and to induce experimental autoimmune encephalomyelitis (EAE) (see 4.10) or for freezing (see 4.8).

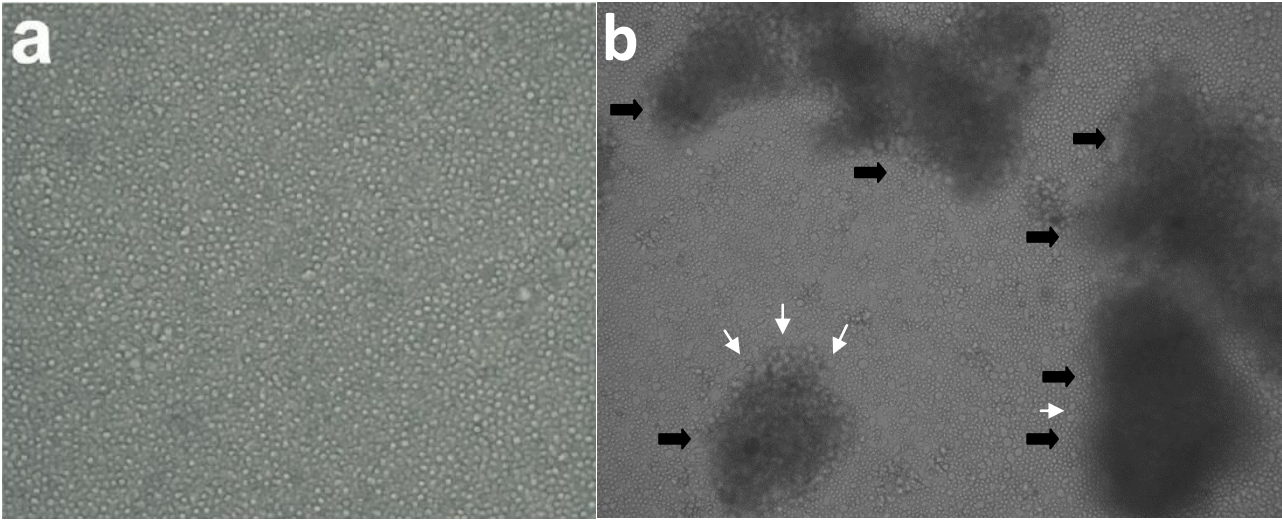


**Figure 11** a) Resting, T-cells. b) Cluster formation of APCs (black arrows) and an increased cell size (white arrow heads) indicate that T-cells became activated.

**Table 4** MBP T-cell lines for EAE induction

MBP T-cell batch	Pathology
MBP T-cell (2008)	classic EAE
MBP T-cell (2009)	classic EAE
LMBP (2012)	GFAP and AQP4 loss
MBP7 (2012)	GFAP and AQP4 loss

## 4.8 Freezing of T-cells

### Materials

- Freezing medium (own stock, see 4.3.2)
- MBP-specific-T-cells (own stock, see 4.7)

### Methods

The cells were transferred to a 50ml Falcon tube and centrifuged (1300rpm, 4°C for 10min). The pellet was resuspended in 2ml of freezing medium and frozen with a cooling rate of -1°C/min to a max of -80°C. Later the T-cells were stored in liquid nitrogen for long term preservation.

## 4.9 Separation of activated lymphocytes and dead or inactive cells trough density gradient centrifugation (optional if needed).

### Materials

- NycoPrep™ 1.077A
- Medium with active, inactive or dead lymphocytes

### Methods

If the amount of dead or inactivated cells in our cell culture was too high they were separated trough density gradient centrifugation from the active T-cells and APCs.

The cells were pooled and centrifuged (1300rpm for 1min/ml, Roomtemperature (RT)). The supernatant was discarded and the pellet was resuspended in 3ml of RPMI-1640. The medium with the cells were layered very carefully over 3ml of NycoPrep™ 1.077A in a 15ml Falcon tube. The samples were centrifuged for 30min (1700 rpm, RT) with a very slow acceleration and deceleration phase. The lymphocytes were then harvested from the interface between RPMI medium and the NycoPrep™ 1.077A solution (Figure 12).The cells were than washed in 4ml of restimulation medium and afterwards centrifuged for 10min (1300rpm, RT). The washing and centrifugation step was repeated and the supernatant was discarded. The pellet was then resuspended in TCGF medium (see 4.2.1) and plated on Ø60mm petri dishes.

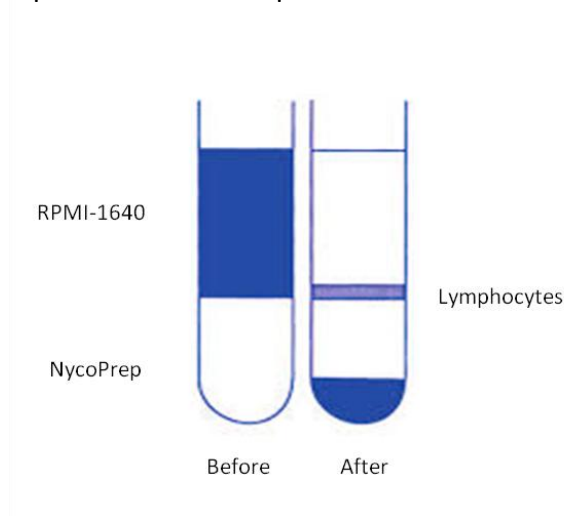


**Figure 12** Cell density gradient. The Lymphocytes were harvested from the interface between RPMI-1640 medium and NycoPrep™ 1.077A solution after centrifugation

## 4.10 EAE induction

### Materials

- MBP-specific-T-cells (Table 4)
- RPMI-1640 (Lonza, BE12-167F)
- 1 X PBS
  - 150mM NaCl (Merck, 1.06404)
  - 250ml Sörensenbuffer
  - 750ml ddH<sub>2</sub>O
- human IgG (Subcuvia, Baxter, G1563300112001)
- NMO-anti-AQP4-IgGs (Table 5)
- 4% PFA (Merck, 1.04005.1000)
  - 40g PFA dissolved in heated 500ml 0.2M Sörensenbuffer
  - Filled up to 1l with ddH<sub>2</sub>O
- 0.2M Sörensenbuffer (pH 7.4)
  - 40mM NaH<sub>2</sub>PO<sub>4</sub> (Merck, 1.06346)
  - 160mM Na<sub>2</sub>HPO<sub>4</sub> (Merck, 1.06580)

**Table 5** *Titers of anti-AQP4 antibodies from patients with NMO used for transfer experiments*

Serum	AQP4 Antibody Titer
J0	1:8192
J1	1:65536
J2	1:16383
RK	1:640
RE	1:10240
GF	1:20480
IgG7	1:2 Mil.
IgG8	1:8 Mil.

### Methods

EAE was induced in Lewis rats (see 4.1) trough intraperitoneal injection of activated MBP-specific-T-cells ( $3.5-7 \times 10^7$  cells per animal) in RPMI-1640 medium. The animals were weight daily and the disease development was scored according to Table 7. Four days after T-cell transfer some animals received an additional intraperitoneal injection 1ml of PBS (control), some received 1ml PBS with

10mg/ml of human IgG (control) or 1ml PBS containing NMO-anti-AQP4-IgG from different human NMO patients (see Table X).

**Table 6** *Number of NMO-IgG containing and control IgG (Subcuvia) in rats with and without MBP T-cell induced EAE*

Treatment	number for pathological analyzed animals (n)
MBP T-cells+IgG J0	24
MBP T-cells+IgG J1	2
MBP T-cells+IgG J2	2
MBP T-cells+IgG RK	2
MBP T-cells+IgG RE	2
MBP T-cells+IgG GF	12
MBP T-cells+IgG 7	13
MBP T-cells+IgG 8	17
MBP T-cells+Subcuvia	30
MBP T-cells+Ø*	46
Ø+NMO IgG**	29

\* Ø= PBS or control IgG( e.g. serum form MS patient)

\*\* NMO IgG= different anti-AQP4 containing sera were used

The animals were sacrificed when they reached an EAE score of 2 (Table 7) and the spinal cords and brains were dissected and fixed in 4% PFA over night at 4°C. After fixation the tissue was embedded in paraffin and Immunohistochemistry (IHC) was performed (see 4.11).

Paraffin embedding was done by our technicians on the basis of well proven standard protocol that will not be included in detail in this master thesis.

**Table 7** *shows scores for EAE symptoms.*

Score	Symptomes
0	no clinical symptoms
0,5	partial loss of tail tonus
1	complete loss of tail tonus
2	hind limb weakness
3	hind limb paralysis
4	hind limb and fore limb paralysis
5	death

## 4.11 Tissue staining methods

### 4.11.1 Immunohistochemistry (IHC)

Immunohistochemistry (IHC) uses specific antibodies that are directed against the epitopes from proteins of interest. In the case of light microscopy a secondary antibody that is conjugated to horse radish peroxidase (POX) is used to detect the first or so called primary antibody. To visualize the construct of the two antibodies diaminobenzidin (DAB) is used to react with the POX. In the case of fluorescence microscopy the secondary antibodies are directly coupled to a fluorophor such as CY2 or CY3.

The EAE rat tissue we used for IHC was paraffin embedded and the material was cut into 3-5µm thick sections.

### 4.11.2 IHC with ABC-System (for light microscopy)

#### Materials

- Coverslip 21x26mm (Carl Roth, H8762)
- Xylol (Sanova, 1306305005)
- EtOH (96%, 70%, 50%) (Brenntag CEE GmbH, 442269)
- Hydrogenperoxidase solution
  - 1ml H<sub>2</sub>O<sub>2</sub> (VWR International GmbH, 1.07210.0250)
  - 150ml methanol (VWR International GmbH, 20847.307)
- 0.2M Sörensenbuffer (pH 7.4)
  - 40mM NaH<sub>2</sub>PO<sub>4</sub> (Merck, 1.06346)
  - 160mM Na<sub>2</sub>HPO<sub>4</sub> (Merck, 1.06580)
- 4% PFA (Merck, 1.04005.1000)
  - 40g PFA dissolved in heated 500ml 0.2M Sörensenbuffer
  - Filled up to 1l with ddH<sub>2</sub>O
- EDTA solution (pH 8.5)
  - 10mM Tris (AppliChem GmbH, A1379)



- 1mM EDTA (Lonza, BE17-161E)
- In ddH<sub>2</sub>O
- TBS (pH 7.6)
  - 10mM Tris (AppliChem GmbH, A1379)
  - 150mM NaCl (Merck, 1.06404)
  - In ddH<sub>2</sub>O
- 0,03% Protease solution
  - 0,015g Protease (bacterial) (Sigma, P8030)
  - In 50ml warm 1 X PBS
- 1 X PBS
  - 150mM NaCl (Merck, 1.06404)
  - 250ml Sörensenbuffer
  - 750ml ddH<sub>2</sub>O
- Scott'solutions
  - 2g KHCO<sub>3</sub> (Merck, 104854) and 20g MgSO<sub>4</sub> (Merck, 105886) in 1000ml dH<sub>2</sub>O
- 10% FCS (Biochrom S01115) in DAKO buffer (DAKO, S3006)
- DAKO buffer (DAKO, S3006)
- Primary antibody (Table 8)
- Secondary antibody (Table 9)
- Avidin- Peroxidase (Sigma, A3151), 1:100 in Dako buffer/ 10% FCS (Biochrom S01115)
- 2% Copper sulfate (Merck, 1.02791)/ 0,9% NaCl
- 25mg/ml 3,3'-Diaminobenzidine (DAB) (Sigma, 32750) in 1 X PBS
- Haemalum (Merck, 1.09249)
- 0,5% HCl (RdH, 30721) in 70% Ethanol
- Eukitt (Kindler R1339)

## Methods

The sections were deparaffinized two times for 15 minutes in Xylol and rinsed twice in 96% EtOH. Afterwards they were put for 30 minutes in a hydrogenperoxidase solution in methanol to block the endogenous peroxidase activity. The sections were then rehydrated in a descending series of EtOH (96%→70%→50%→dH<sub>2</sub>O) and washed three times in Tris buffered Saline (TBS).

Different epitop retrieval procedures were used depending on the antigen. The sections were not treated or treated either for one hour in Ethylenediaminetetraacetic acid (EDTA) solution pH 8,5 in a household food steamer device (Multi Gourmet FS 20, Braun, Germany) and washed three times in PBS or incubated for 15min in 0,03% Protease (in warm PBS, 37°C) and washed three time in cold PBS (4°C). After this step the nonspecific binding sites were blocked for 20min with 10% FCS solution in a humid chamber at room temperature. After the blocking step the sections were incubated over night with the primary antibody in 10% FCS/DAKO buffer at 4°C.

The slides were washed again with TBS and the sections were incubated with biotinylated secondary antibodies in 10FCS/DAKO buffer for one hour at room temperature. Afterwards the slides were rinsed three times in TBS and avidin-peroxidase 1:100 in 10%FCS/DAKO buffer was incubated for one hour at room temperature. The slides were rinsed three times in PBS and developed in 0,5mg/ml DAB in 50ml PBS/0,01%H<sub>2</sub>O<sub>2</sub> solution.

The Section were counterstained with haemalaun eosin for 8 seconds than washed in water, differentiated in 0,5% hydrochloric acid ethanol and washed with water again. Afterwards the tissue was blued in scott's solution for 5 minutes, washed with water and dehydrated in EtOH (dH<sub>2</sub>O →50%→70%→96%). Finally the slides were kept in ester until they were embedded in eukit.

**Table 8** *list of primary antibodies*

Primary Antibody	Antibody Type	Target	Dilution	Pre treatment	Source
GFAP	Rabbit, pc	filaments of mature astrocytes	1:3000	EDTA pH 8,5	DAKO Z0334
AQP4	Rabbit, pc	Aquaporin 4	1:250		Sigma, A5971
Iba-1	Rabbit, pc	microglial and macrophages ionized Ca <sup>2+</sup> -binding protein	1:3000	EDTA pH 8,5	Wako Pure Chemical Industries, 019-19-741
C9neo	Rabbit, pc	activated lytic complement componets	1:2000	0,03% Protease	GE Healthcare/Amersham
CD3Nm	Rabbit, mc	early T-cell antigen	1:2000	EDTA pH 8,5	Thermo Scientific, RM 9107
W3/13	Mouse, mc	T-cells and granulocytes	1:50	Citrat buffer pH6	Harlan Sera-Lab, MAS010b
humIgG	Rabbit, pc	gamma-chains of human IgG	1:500	0,03% Protease	DAKO
ED1	Mouse, mc	macrophages and weakly by peripheral blood granulocytes	1:10000	EDTA pH 8,5	AbD Serotec
PLP	Rabbit, pc	Proteolipid Protein	1:250	EDTA pH 8,5	Sara Piddlesten
MBP	Rabbit, pc	Myelin Basic Protein	1:2500		DAKO A0623
CNPase	Mouse, mc	oligodendrocytes in the grey and white matter	1:2000	EDTA pH 8,5	Sternberger Monoclonals, SMI91
Ox6	Mouse, mc	MHC2 molecules	1:500	EDTA pH 8,5	AbW Serotec, MCA46G
GrB	Rabbit, pc	Cytoplasmic granules of cytolytic T-lymphocytes and natural killer cells	1:50	EDTA pH 8,5	Abcam, ab4059

**Table 9** *list of secondary antibodies*

Secondary Antibodies	Target	Dilution	Source
Donkey-bi- $\alpha$ -Rabbit	Rabbit Ig	1:2000	Jackson
Sheep-bi- $\alpha$ -Mouse	Mouse Ig	1:500	Jackson

### 4.11.3 Double staining for fluorescence microscopy

#### Materials

- Coverslip 21x26mm (Carl Roth, H8762)
- Xylol (Sanova, 1306305005)
- EtOH (96%, 70%, 50%) (Brenntag CEE GmbH, 442269)
- Hydrogenperoxidase solution
  - 1ml H<sub>2</sub>O<sub>2</sub> (VWR International GmbH, 1.07210.0250)
  - 150ml methanol (VWR International GmbH, 20847.307)
- 0.2M Sörensenbuffer (pH 7.4)
  - 40mM NaH<sub>2</sub>PO<sub>4</sub> (Merck, 1.06346)
  - 160mM Na<sub>2</sub>HPO<sub>4</sub> (Merck, 1.06580)
- 4% PFA (Merck, 1.04005.1000)
  - 40g PFA dissolved in heated 500ml 0.2M Sörensenbuffer
  - Filled up to 1l with ddH<sub>2</sub>O
- EDTA solution (pH 8.5)
  - 10mM Tris (AppliChem GmbH, A1379)
  - 1mM EDTA (Lonza, BE17-161E)
  - In ddH<sub>2</sub>O
- TBS (pH 7.6)
  - 10mM Tris (AppliChem GmbH, A1379)
  - 150mM NaCl (Merck, 1.06404)
  - In ddH<sub>2</sub>O
- 1 X PBS
  - 150mM NaCl (Merck, 1.06404)
  - 250ml Sörensenbuffer
  - 750ml ddH<sub>2</sub>O
- DAKO buffer (DAKO, S3006)

- DAKO diluents (DAKO, S2022)
- Primary antibody (Table 9)
- Secondary antibody (Table 10)
- Gelto
  - 6g glycerine (Gibco BRL, 15514-011)
  - 2,4g Mowiol (CalbioChem, 475904)
  - 12ml Tris 0,2M pH 8,5 (AppliChem, A1379)
  - 6ml dH<sub>2</sub>O
  - Stirred for 10 minutes at 50°C, centrifuge at 5000g for 15 minutes
- 0,1M Gallate (Sigma, P3130) in Gelto

### Methods

3-5µm tick EAE rat sections were deparaffinized, the endogenous peroxidase activity was blocked and the sections were rehydrated as described above in the ABC-system.

The sections were treated for antigen retrieval for one hour in Ethylenediaminetetraacetic acid (EDTA) solution in a household food steamer device (Multi Gourmet FS 20, Braun, Germany).

After the epitope retrieval the slides were rinsed three times in TBS and the nonspecific binding sites were blocked for 30min with DAKO diluent in a humid chamber at room temperature.

After the blocking step the sections were incubated over night with the primary antibody in DAKO diluent buffer at 4°C.

The secondary antibodies were directly conjugated to a fluorophore and they were incubated for one hour at room temperature. For some delicate antibodies the signal was enhanced by incubation with biotinylated secondary antibody followed by incubation with a Streptavidin coupled fluorophore. Afterwards the sections were rinsed in dH<sub>2</sub>O and mounted with Gallate-Geltol.

Cells were examined at Leica TCS SP5 LASAF microscope (Leica Microsystems, CMS-GmbH, Germany) with an argon-laser and a DPSS561 laser.

**Table 10** *list of double stainings*

Primary Antibody	Antibody Type	Target	Dilution	Pretreatment	Secondary antibody	Dilution
Ox8 + GrB	Mouse, mc  Rabbit, pc	CD8α  Cytoplasmic granules of cytolytic T-lymphocytes and natural killer cells	1:100  1:50	EDTA pH 8,5	hsαmDL488  bi-α-R J + StrDL549	1:100  1:2000 1:200
GFAP + Ox6	Rabbit, pc  Mouse, mc	filaments of mature astrocytes MHC2 molecules	1:1500  1:125	EDTA pH 8,5	dαRCy3  bi-α-m J + StrCy2	1:200  1:500 1:100

**Table 11** *list of fluorophor coupled secondary antibodies*

fluorophor coupled secondary antibodies	Dilution
hsαmDL488	1:100
bi-α-R J + Str DL549	1:2000 + 1:200
dαRCy3	1:200
bi-α-m J + StrCy2	1:500 + 1:100

#### 4.11.4 Haemalaun (Haematoxylin)-Eosin staining

##### Materials

- Coverslip 21x26mm (Carl Roth, H8762)
- Xylol (Sanova, 1306305005)
- EtOH (96%, 70%, 50%) (Brenntag CEE GmbH, 442269)
- Haemalum (Merck, 1.09249)
- Scott'solutions
  - 2g KHCO<sub>3</sub> (Merck, 104854) and 20g MgSO<sub>4</sub> (Merck, 105886) in 1000ml dH<sub>2</sub>O
- Eosin staining solution
  - 10g eosinY (yellowish) (Merck, 115935) in 100ml H<sub>2</sub>O
- 0,5% HCl (RdH, 30721) in 70% Ethanol
- Eukitt (Kindler R1339)

## Methods

The sections were deparaffinized two times for 15 minutes in Xylol and rinsed twice in 96% EtOH. Afterwards they were rehydrated in a descending series of EtOH (96%→70%→50%→dH<sub>2</sub>O). Then the sections were incubated for five minutes in Haemalaun, rinsed three times in tap water, differentiated for five seconds in acid alcohol and rinsed again three times in tap water. Afterwards the sections were put for five minutes in Scott's solution, washed in tap water, counterstained with 1% Eosin solution for three minutes and dehydrated them in an ascending series of EtOH (50%→70%→96%). Finally the samples were mounted with Eukitt and glass cover slips.

### **4.11.5 Klüber-Pas staining**

#### Materials

- Coverslip 21x26mm (Carl Roth, H8762)
- Xylol (Sanova, 1306305005)
- EtOH (96%, 70%, 50%) (Brenntag CEE GmbH, 442269)
- Eukitt (Kindler R1339)
- 0,1% Luxol Fast Blue
  - 1g Luxol Fast Blue (Chroma/Szabo, 1B389) in 1000ml 96% EtOH at 57°C overnight
- Sulfit washing solution
  - 2ml 10% KHSO<sub>3</sub> (Sigma, P2522) and 0,5ml conc. HCl (RdH, 30721) in 100ml dH<sub>2</sub>O
- 0,1% Lithiumcarbonat (Merck, 105680) in dH<sub>2</sub>O
- 0,8% Periodic acid (Merck, 100524) in dH<sub>2</sub>O
- Schiff's reagent (Merck, 1.09033)
- 

#### Methods

The samples were dewaxed two times for 15 minutes in Xylol and rinsed twice in 96% EtOH. Then they were put directly in 0,1% Luxol Fast Blue at 57°C over night. After cool down the sections were rinsed in 96% EtOH and washed in dH<sub>2</sub>O. The sections were put afterwards in 0,1% Lithiumcarbonate solution for 5 min and then in 70% EtOH until the grey and white matter is clearly distinguished from each other (myelin sheaths remains stained). Then the slides were washed in

dH<sub>2</sub>O, oxidized in 0,8% Periodic acid for 10 minutes, washed again in dH<sub>2</sub>O, treated with Schiff's solution and washed three times for two minutes each in Sulfit solution. The sections were finally washed in tap water for five minutes, dehydrated in an ascending series of EtOH (50%→70%→96% ) followed by n-butylactate and mounted with Eukit.

#### **4.11.6 Bielschowsky staining**

##### Materials

- Coverslip 21x26mm (Carl Roth, H8762)
- Xylol (Sanova, 1306305005)
- EtOH (96%, 70%, 50%) (Brenntag CEE GmbH, 442269)
- Eukitt (Kindler R1339)
- Development solution
  - 1 drop conc. HNO<sub>3</sub> (Merck, 100443), 0,5g Citric acid (Sigma/Fluka, 27488) in 20ml Formalin (Merck, 1.04003.1000)
- 10% Silver nitrate solution
  - 10g silver nitrate (Merck, 1.09033) in 100ml dH<sub>2</sub>O
- 5% Sodiumthiosulfat (Merck, 106516) in dH<sub>2</sub>O
- 25% NaOH Merck, 106580) in dH<sub>2</sub>O

##### Methods

The sections we were deparaffinized two times for 15 minutes in Xylol and rinsed twice in 96% EtOH. Afterwards they rehydrated in a descending series of EtOH (96%→70%→50%→dH<sub>2</sub>O). Afterwards silver nitrate solution was put for 20 minutes on the slides and collected afterward in a flask. The samples were rinsed in dH<sub>2</sub>O. Drop by drop of concentrated HNO<sub>3</sub> was added in the flask with the silver nitrate solution, the solution was mixed well after each drop until the precipitate is dissolved. Afterwards two more drops of concentrated ammonia were added to the silver nitrate solution and the slides were incubated with the solution for 15 minutes in the dark. The sections were washed then two times in dH<sub>2</sub>O with two drops of concentrated HNO<sub>3</sub> and incubated again in nitrate-ammonia-solution with three drops of development solution. After 3 to 5 minutes the axons are stained black and the background is stained yellowish. The samples were rinsed in dH<sub>2</sub>O, fixed in 5% sodiumthiosulfate solution for three minutes and rinsed again in dH<sub>2</sub>O. After dehydration in

an ascending series of EtOH (50%→70%→96%) the slides were put in n-butyl lactate and mounted with Eukit afterwards.

## **4.12 Quantification**

### **4.12.1 Semi quantitative scoring**

Analysis of immunohistochemically stained cortex sections was performed by light microscopy. The semi quantitative scoring was done for activated microglia of animals injected with different NMO-IgG sera and their controls. The surface of 142 whole Cortex sections was examined for cortical inflammation of microglia and scored. Therefore the width (1, 2, 3, 4) of cortical immunoreactivity for Iba-1 was multiplied by the extent of invasion of the microglia into the cortex up to the third cortical layer (meninges=1, C1=2, C2=3 and C3=4).

### **4.12.2 Quantitative analysis**

Detailed analysis of 43 GFAP and AQP4 stained spinal cord sections. These sections were scanned with the Aperio Technologies slide scanner (SN: SS005018) with a 400 times magnification. The quantification of these slides was performed with the Aperio ImageScope v. 12.0.0.5039 program. Therefore the whole sections and the areas of GFAP and AQP4 loss (lesions) were exactly measured in  $\mu\text{m}^2$  with the “negative pen tool”. Afterward the measured areas of the lesions were divided through the areas of the whole sections and multiplied with 100 to get the percentage of the lesion areas on the sections. Further the Kruskal-Wallis statistic test was used as a global screening test to see if any possible pairwise group comparison shows a significant difference in the distribution of the given marker. A  $p\text{-value} \leq 0.05$  was considered as statistically significant. Statistical analyses were performed using PASW Statistics 18 (SPSS Inc.)



## 5. Results

### 5.1 Basic pathology of NMO-like lesions induced by NMO IgG in combination with encephalitogenic T-cell in Lewis rat model.

The injection of AQP4 specific antibodies in EAE rats induces lesions with astrocyte damage in the spinal cord. These lesions are characterized by foregoing AQP4 and further GFAP loss follows, extensive immunoglobulin and complement deposition on astrocytic foot processes around the blood vessels, granulocytic infiltrates, the presence of T-cells and activated microglia/macrophages with no demyelination (Bradl et al., 2009) (Figure 13).

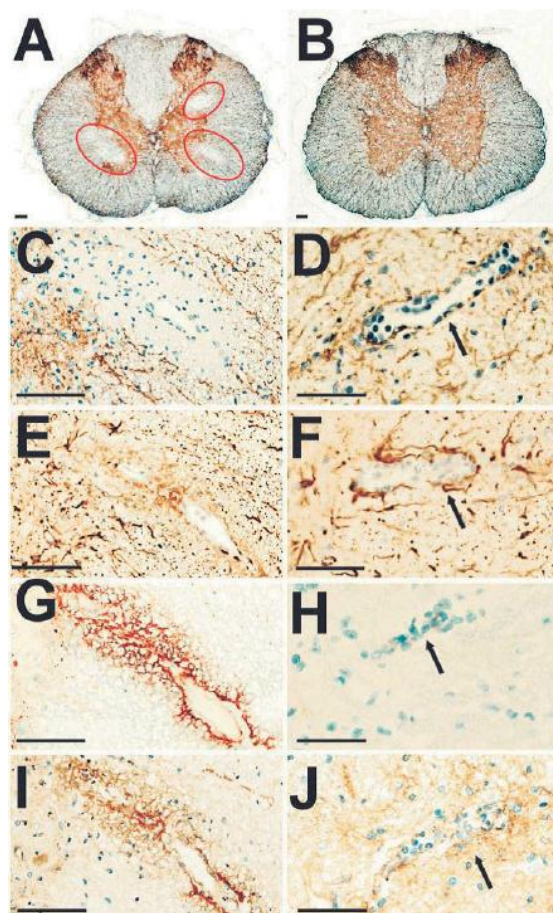


**Figure 13** Spinal cord cross sections of animals injected with T-cells and human anti-aquaporin-4 (anti-AQP4) antibodies (A, C, E, G, I) or T-cells and control IgG (B, D, F, H, J). The sections were reacted with the commercial anti-AQP-4 antibody (A, B; detailed in C, D), or antibodies against glial fibrillary acidic protein (GFAP; E, F), C9 (G, H), and human IgG (I, J). Areas of AQP4 loss are encircled in red. Arrows point to a perivascular inflammatory cuffs. Transfer of neuromyelitis optica (NMO) immunoglobulin in experimental autoimmune encephalomyelitis (EAE) results in profound loss of AQP4 (A, C) and GFAP (E), as well as massive C9 (G) and immunoglobulin deposition (I) around inflamed vessels predominantly in the spinal cord gray mater. In contrast, transfer of control immunoglobulin shows inflammation with preservation of perivascular AQP-4 (B, D) and GFAP (F) reactivity, no C9 deposition (H), and diffuse immunoglobulin staining (J) around inflamed vessels. Scale bar 300µm. Picture and legend are taken from (Bradl et al., 2009)

## **5.2 In the cortex of EAE rats human anti-aquaporin antibodies induce stronger microglia activation than subcuvia or T-cells alone.**

A recent study described astroglia damage in the first cortical layer but preserved GFAP and AQP4 signal in the underlying layers in the brains of NMO patients. Additionally, strong microglia activation in the second cortical layer and significant loss of cortical neurons was described (Saji et al., 2013).

To find out if the same microglia activation pattern can be seen in animal model, the meninges and the first three cortical layers (C1, C2 and C3) were analyzed. Thereby, a semi quantitative scoring system (see Materials and Methods) for the evaluation of sections stained by immunocytochemistry with the microglia marker Iba-1 was used.

NMO-IgG sera from eight different NMO patients with high titers (Table 5) were injected in MBP-specific T-cell induced EAE rats. As control either Lewis rat treated with NMO-IgG without the induction of EAE or EAE rats treated with subcuvia, PBS or sera that contained no NMO-IgG were analyzed.

To find out which of the sera induces the strongest inflammation in the EAE rat cortex the animals were sacrificed 24h after injection with the different sera containing anti-AQP4 antibodies. The cortex sections were stained under same conditions with the microglia marker Iba-1 and the activated microglia were distinguished from the non-activated through aggregation stages and morphological alterations of the cell body and the processes (Figure 14 A-D).

Differences in microglia activation could be detected between the EAE animals treated with the different NMO-sera whereas the EAE rats treated with IgG J0, IgG GF, IgG7 and IgG8 displayed very high and comparable microglia activation. In some cases EAE rats treated with subcuvia or no anti-AQP4 antibodies showed high microglia activation. Controls without T-cell mediated inflammation showed no increased immunoreactivity in comparison to controls. Furthermore, it was observed that within the group of each serum the macrophage/microglia activation increases with time after EAE induction and antibody transfer (Figure 15).

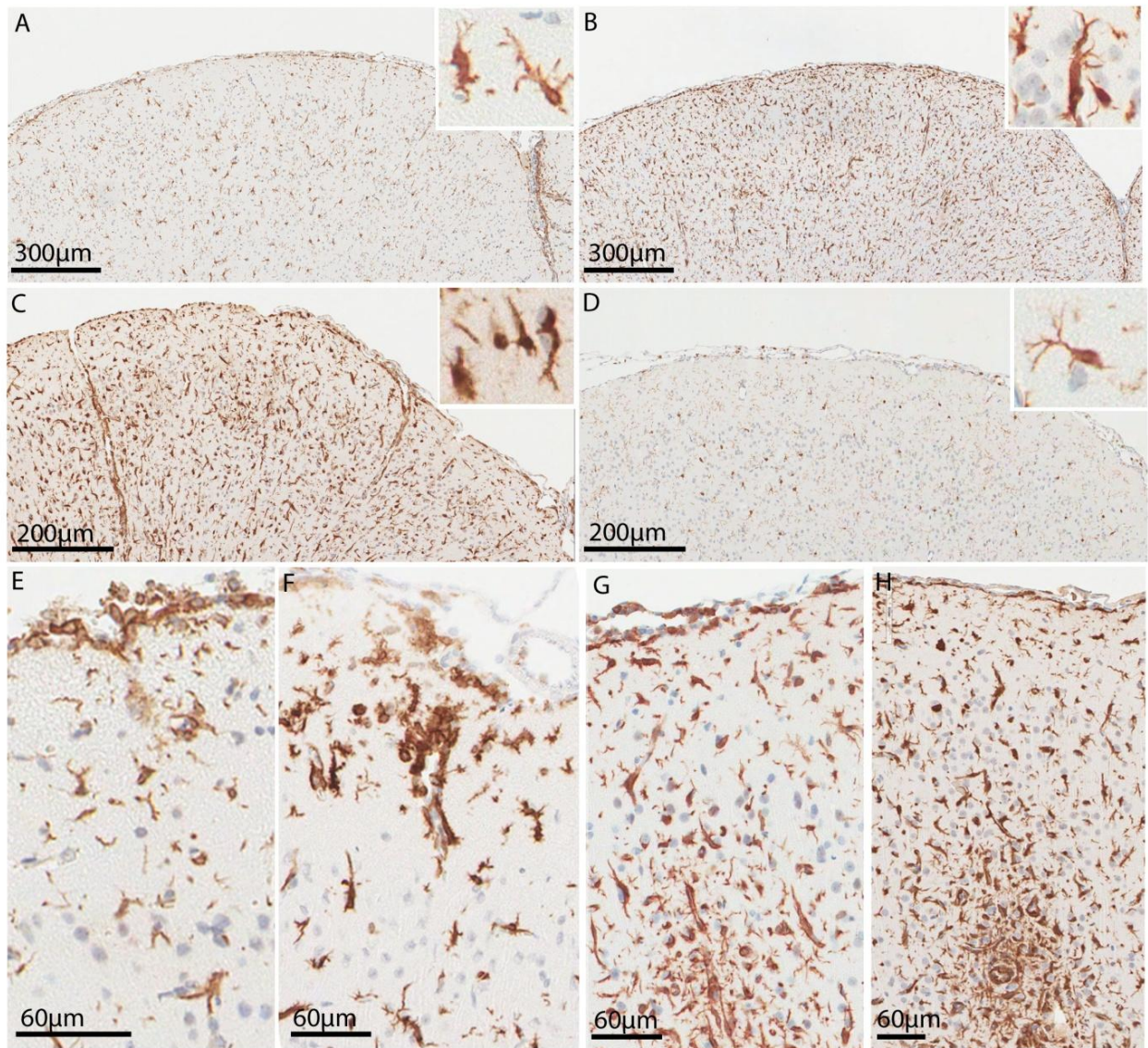


**Figure 14** Cortex cross sections of animals injected with MBP-specific T-cells and human serum containing anti-AQP4 antibodies (A, B, C,) or control groups (D); Inflammation displayed in different cortical layers: meninges (E), cortical layer one =C1 (F), cortical layer two=C2 (G) and cortical layer three=C3 (H); The sections were immunohistochemically stained with the commercial Iba-1 antibody. (A) Microglia activation just in the meninges (E) and C1 (F); (B) Microglia activation in C1 (F), C2 (G), C3 (H) and the meninges (E); (A and B) Difference between NMO IgG sera which induce weak (A) and strong (B) microglia activation after 24h; (C) 72h with NMO-IgG treated EAE animal. Microglia activation and perivascular inflammatory cuffs can be seen in high appearance in the whole section (E,F,G and H); (B and C) A progression of the inflammation can be seen in EAE rats treated with the same NMO-IgG serum for 24h (B) and 72h (C). (A, B and C, insert) Activated microglia with swollen cell bodies and thickened processes. (D, inset) Resting microglia with normal appearing cell body and very fine branching of the cell processes.

Lesions in the cortex could be documented in EAE rats treated for 48h with IgG GF (Figure 15). All other animals treated with different sera as well as controls show no astrocyte damage despite the strong microglia activation in some cases (Figure 15). Further, minor to

moderate T-cell infiltration was present in the meninges and the first three cortical layers (Figure 16 v-w) but did not correlate with the degree of microglia activation.

Although astrocyte loss occurred when treating with two of the NMO IgG sera, none of the lesions were in the first cortical layer. So the animal model cannot reflect the astroglia pathology described by Saji et al (Saji et al., 2013) in NMO patients.

After 24h the EAE animals treated with the J0 IgGs showed moderate to strong microglia activation combined with AQP4 loss and astrocyte damage in some of the cortices. After 72h massive inflammation with strong AQP4 and GFAP loss could be observed.

In contrast to the cortex, lesion frequently appeared in the spinal cord (Data not shown) of EAE animals treated with different NMO IgG sera and they were comparable to those described before by Bradl et al (Bradl et al., 2009).

As mentioned above IgG J0 displayed lesions in the cortex but also in the spinal cord of 24h treated EAE rats. IgG7, IgG8 and IgG GF showed moderate astrocyte loss in the spinal cord after 24h. The astrocyte damage in the spinal cord increased with the anti-AQP4 antibodies in most of the EAE rats after 48h of incubation. This can be associated to the activation of microglia. In the 48h subcutaneous treated EAE rats AQP4 and GFAP loss was minor or absent. The T-cell treated rats showed weak to moderate microglia activation and no astrocyte damage. The Lewis rats treated just with the NMO IgGs showed neither inflammation nor AQP4 or GFAP loss



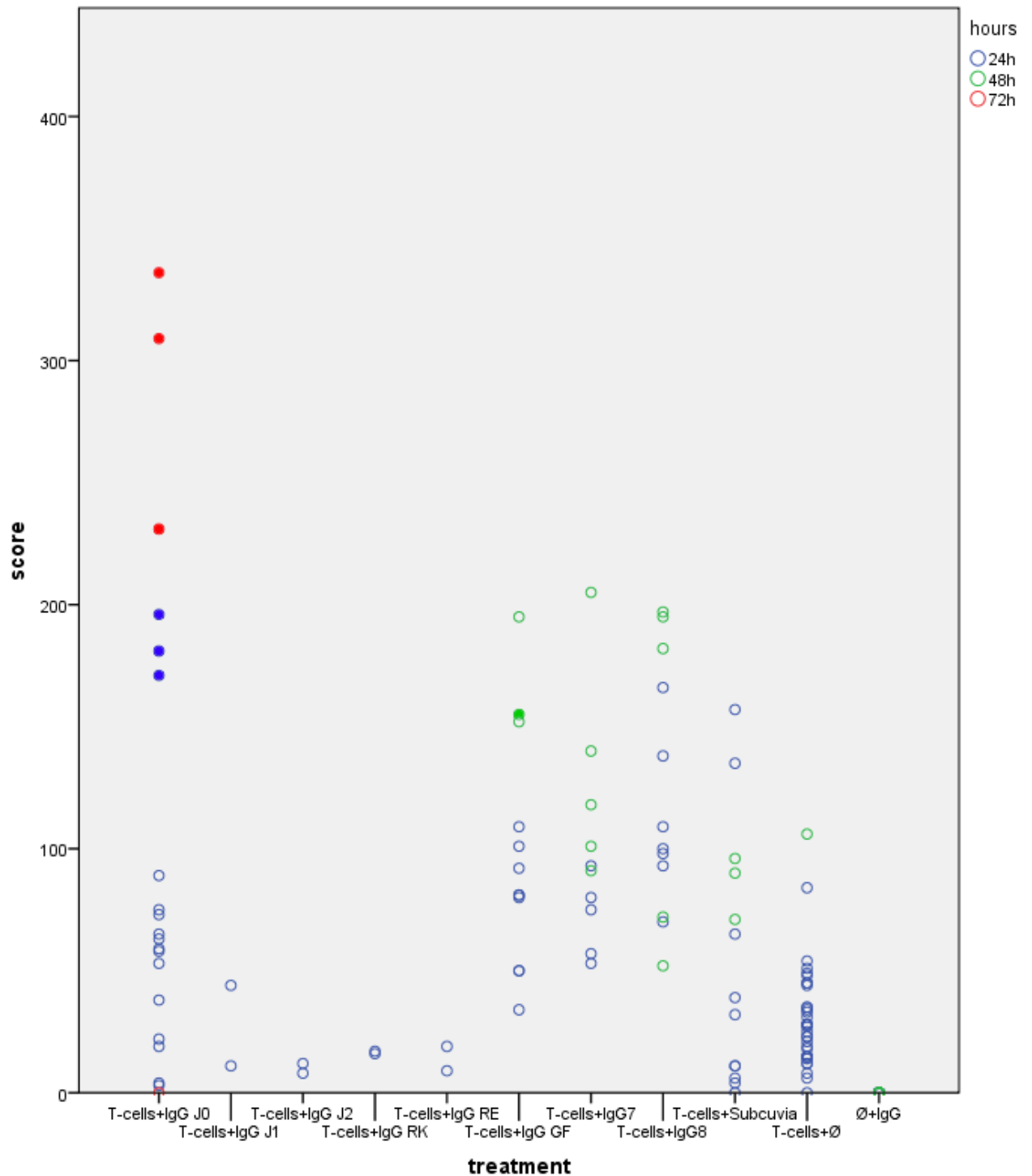


**Figure 15** *Iba-1* cortical activation score for EAE rats treated with different NMO-IgG sera (J0=n20, J1=n2, J2=n2, RK=n2, RE=n2, GF=n12, 7=n10 and 8=n12) and controls (Subcuvia=n13, T-cells+Ø=35, Ø+IgG=n32); A filled circle displays astocyte loss in the cortex; EAE animals with injected IgG-J0, IgG-GF, IgG7 and IgG8 display the highest inflammation scores increasing with the duration of the anti-AQP4 antibody treatment; The MBP T-cell treated animals which did not receive human-NMO serum showed a variable degree of inflammation intensity and microglia/macrophage activation in the case of control IgG (subcuvia) co-transfer; Lewis rats without T-cell mediated EAE showed no macrophage/microglia activation

### **5.3 Detailed description of cortical lesion pathology induced by NMO IgG in EAE rats.**

To analyze the process of immune system activation and the influence of different immune cells during cortical NMO-like lesion formation the Iba-1 marker was used to stain microglia, the CD3 marker for T-cells, the C9 marker to display complement activation and the human IgG marker for detection of the injected NMO or control IgG in rat cortex tissue from animals sacrificed at different time points (24h, 48h and 72h) after NMO-IgG serum injection.

In all cases treated with NMO IgG that displayed AQP4 loss (Figure 16 e,g) and astrocyte degeneration (Figure 16 i,k), the lesion formation was coupled to occurrence of T-cells (Figure 16 u,w), activation of perivascular microglia (Figure 16 q,s) and complement deposition associated (Figure 16 m) to human anti-AQP4 antibodies around inflamed vessels at early time points after antibody transfer (Figure 16 A, C, a, c). However, 72h after the injection of human NMO-IgG no or very weak complement signals was seen (Figure 16 o) in contrast to the 24h treated animals (Figure 16 m). Furthermore, EAE rats with low anti-AQP4 antibody diffusion into the cortex (Figure 16 B,b) showed no AQP4 and GFAP loss (Figure 16 f,j) after 48h of NMO-IgG treatment, despite the presence of activated microglia (Figure 16 r) and T-cells (Figure 16 v). EAE animals with NMO IgG serum treatment but with more profound blood brain barrier injury and human IgG leakage in the cortex showed GFAP and AQP4 loss already 24h after antibody transfer (Figure 16 A, a, e, i). Additionally, complement signal in EAE rats with poor cortical NMO IgG penetration appears diffusely within the tissue rather than vessel associated (Figure 16 n).

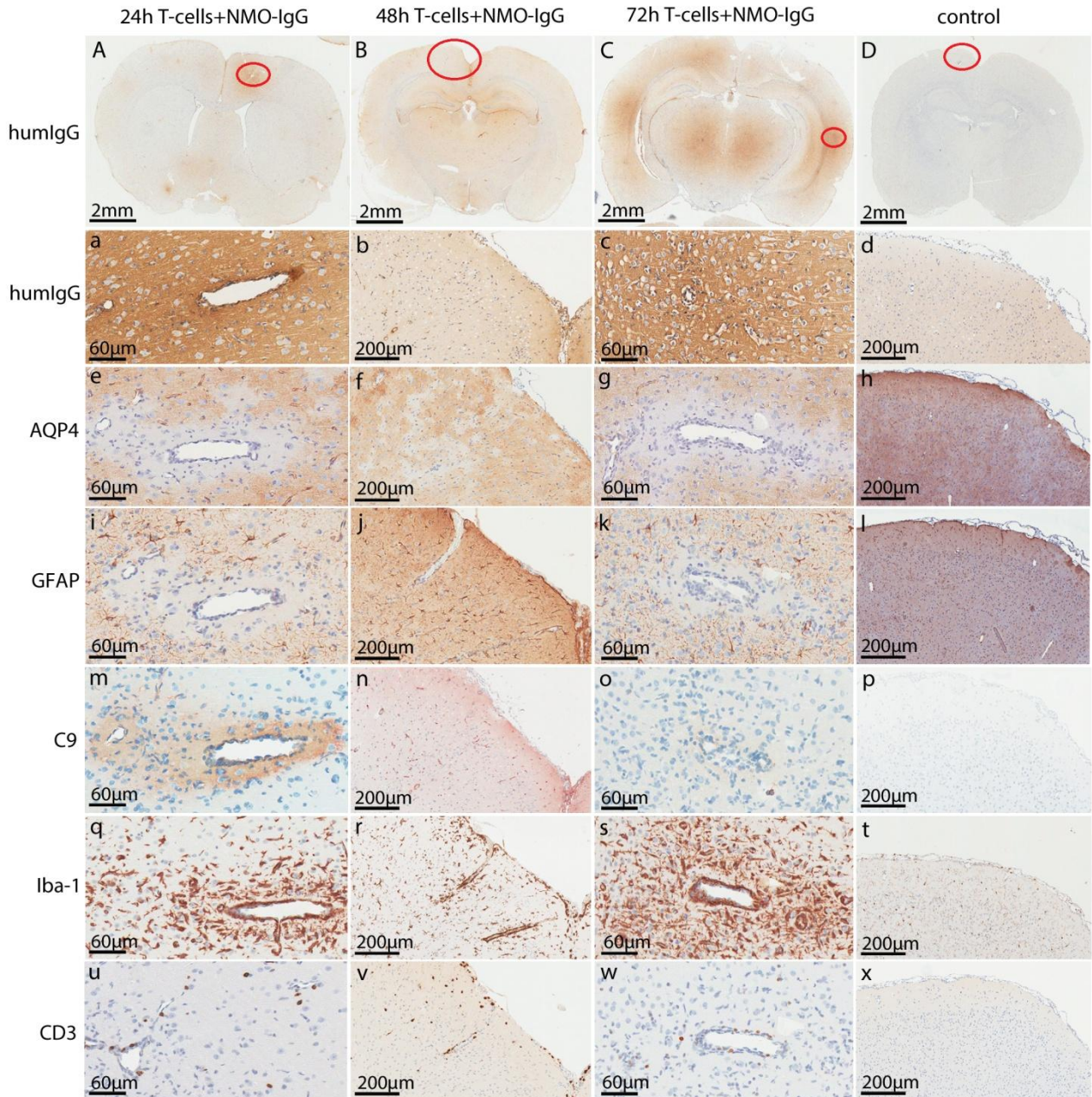


**Figure 16** Cortex cross sections of animals injected with MBP T-cells and the human serum containing anti-AQP4 antibodies (A, B, C,). Control groups are representative for EAE animals without and with subcutaneous treatment (D). Areas that were analyzed are encircled in red; Antibody diffusion in the cortex is animal (A, a and B, b) and time (A, a and C, c) dependent; EAE animals with high NMO-IgG concentrations in the cortex (a and c) display AQP4 (e and g) and GFAP (i and k) loss; EAE animals with low anti-AQP4 antibody titers in the cortex (b) display no AQP4 (f) and GFAP (j) loss; AQP4 and GFAP loss is accompanied additionally with anti-AQP4 antibody presence, with complement activation (m and o), microglia infiltration (q and s) and the occurrence of T-cells (u and w); EAE rats with low NMO-IgG concentrations in the cortex display diffuse complement fixation (n) and no AQP4 and GFAP loss despite the activation of microglia (r) and the presence of T-cells (v). Control rats show neither astrocyte damage (h and l) nor any traces of immune system activation (p, t and x)



## 5.4 AQP4 and GFAP loss is induced in EAE after transfer of selected MBP reactive T-cell lines in the absence of pathogenic antibodies.

Some EAE rats displayed very atypical lesions in the spinal cord (Figure 17 B and C) and the medulla oblongata (data not shown) but not in the cerebral cortex (data not shown). These lesions were in contrast to classical NMO lesions (Figure 17 A) not centered by blood vessels. They affected large areas of the spinal cord (Figure 18) as well as the medulla (data not shown).

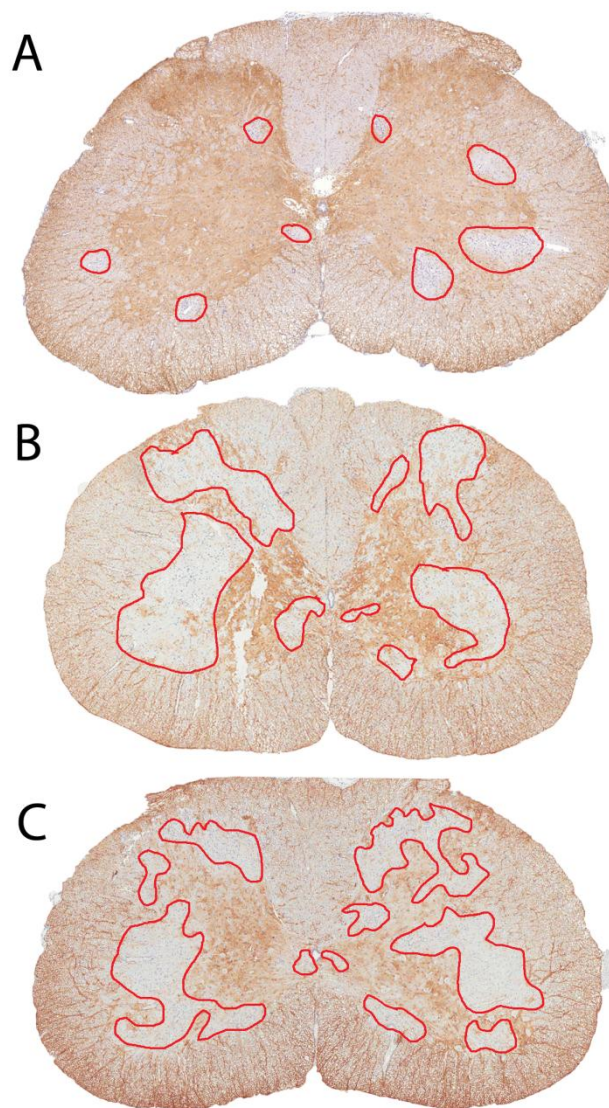


**Figure 17** Spinal cord cross sections of EAE animals induced with two different MBP T-cells lines (A, B, C) and human serum containing anti-AQP4 antibodies (A and B) or PBS (C); Areas of AQP4 loss are encircled in red; 2008 MBP T-cell line to induce EAE and following treatment with human NMO serum. Typical NMO lesion is displayed in (A); LM BP7-MBP T-cell line to induce EAE is displayed in (B and C). (B) was treated with human NMO serum (C) was treated with PBS. The AQP4 loss (B and C) show no sharp border and affect large areas in the spinal cord grey matter in non serum treated (C) anti-AQP4 antibody treated (B) animals.



Since such lesions we first observed in animals injected with human NMO sera, which contained very high antibody titers (IgG7 1:2Mil and IgG8 1:8Mil), it was believed that these lesions were antibody mediated. However similar lesions were also present in the same experiments in control EAE rats treated with subcuvia or PBS (Figure 17 C). In antibody-mediated lesions as well as in these particular lesions GFAP and AQP4 loss increased with time (Figure 18). To see any discrepancy between the EAE animals treated with human NMO serum and the control EAE animals the lesion sizes was measured and quantified with the Aperio ImageScope program (see Materials and Methods 4.12.2) (Figure 18). The difference between the groups was analyzed with the Kurskal-Walles Test. No differences in lesion size were seen in NMO IgG treated and control antibody treated animals.

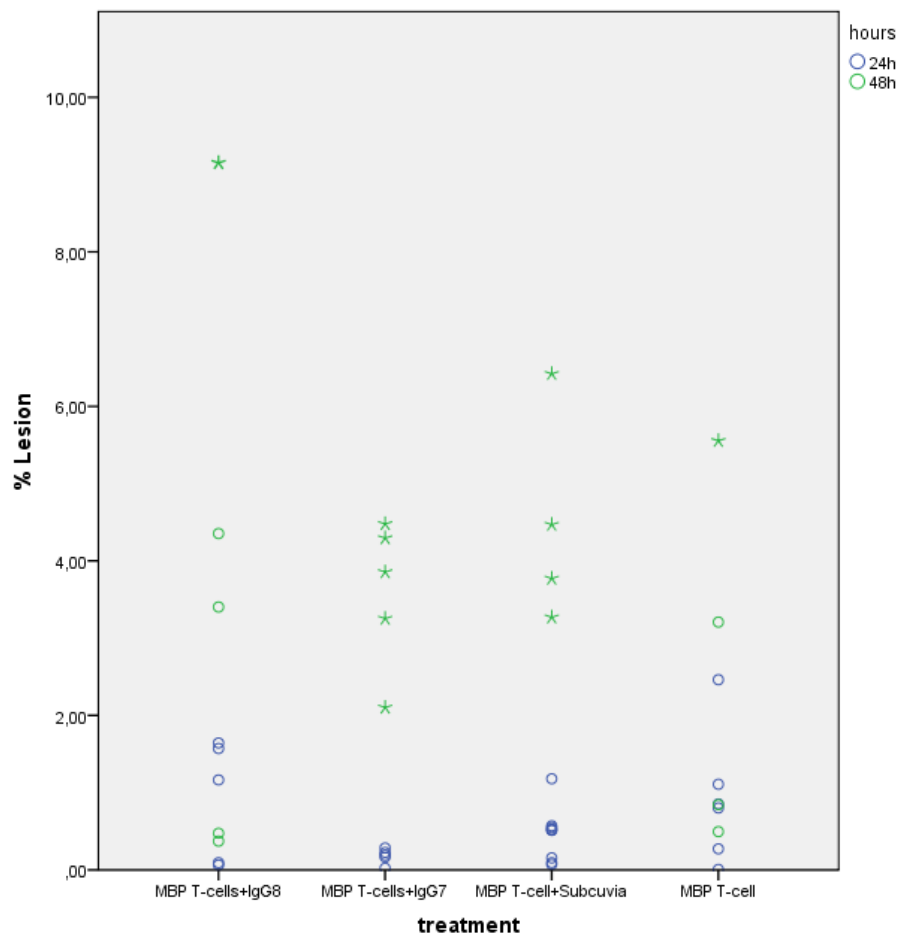


**Figure 18** Quantitative analyses of AQP4 loss for EAE rats treated 24h and 48h with different NMO-IgG sera (IgG7=n10 and IgG8=n10) and controls (Subcuvia=n13, PBS=n10). An asterisk describes appearing vacuolization in lesions; all groups display AQP4 loss that increases with time; all groups display at least one case of vacuolization.

These data indicates that the particular MBP reactive T-cell lines, used in these experiments were able to induce inflammatory brain and spinal cord lesions with profound astrocyte damage. Since such lesions have not been described before in other EAE models (Aboul-Enein et al., 2004; Ben-Nun et al., 1981; Gold et al., 2006) ), induced by CNS-reactive T-cell lines a detailed immunopathological analysis was performed to get insight into the mechanisms responsible for their formation.

## **5.5 Tissue vacuolization (spongy degeneration) precedes AQP4 and GFAP loss in T-cell mediated EAE lesions.**

Additionally, to the large surface of the lesions mentioned above vacuolization in early stages of lesion formation in the NMO IgG treated and non treated MBP T-cell induced EAE rats could be observed. To characterize this lesion type and the vacuolization immunocytochemistry for immune system components, demyelination and axonal degeneration was performed. Thereby, it was confirmed that the lesions with profound AQP4 (Figure 19 A-C and a-c) and GFAP (Figure 19 E-G and e-g) loss and vacuolization occurred in EAE animals treated with (Figure 19 M,N and m,n) and without human NMO serum (Figure 19 O and o). Granulocyte infiltrations in the respective lesions were variable (Figure 19 I-K and i-k). and C9 reactivity was absent or occasionally seen in small granules, which were not associated with the blood vessels (Figure 19 Q, q, Figure 19 R,S and r,s). In all lesions strong microglia activation (Figure 20 A-C, a-c and E-G, e-g), high numbers of MHC II expressing cells (Figure 20 Q-S and q-s), large numbers of CD3 positive T-cells (Figure 20 I-K and i-k) and cytotoxic T-cells, expressing granzyme B (Figure 20 M-O and m-o) could be found. In contrast to the dominant astrocyte loss very little to no myelin loss could be detected with chemical staining (Figure 21 A-C and a-c) and with markers for myelin basic protein (MBP) (Figure 21 E-G and e-g), myelin proteolipid protein (PLP) (Figure 21 I-K and i-k) and oligodendrocytes (ODC) (Figure 21 Q-S and q-s). Finally no axon damage could be found (Figure 21 M-O and m-o).

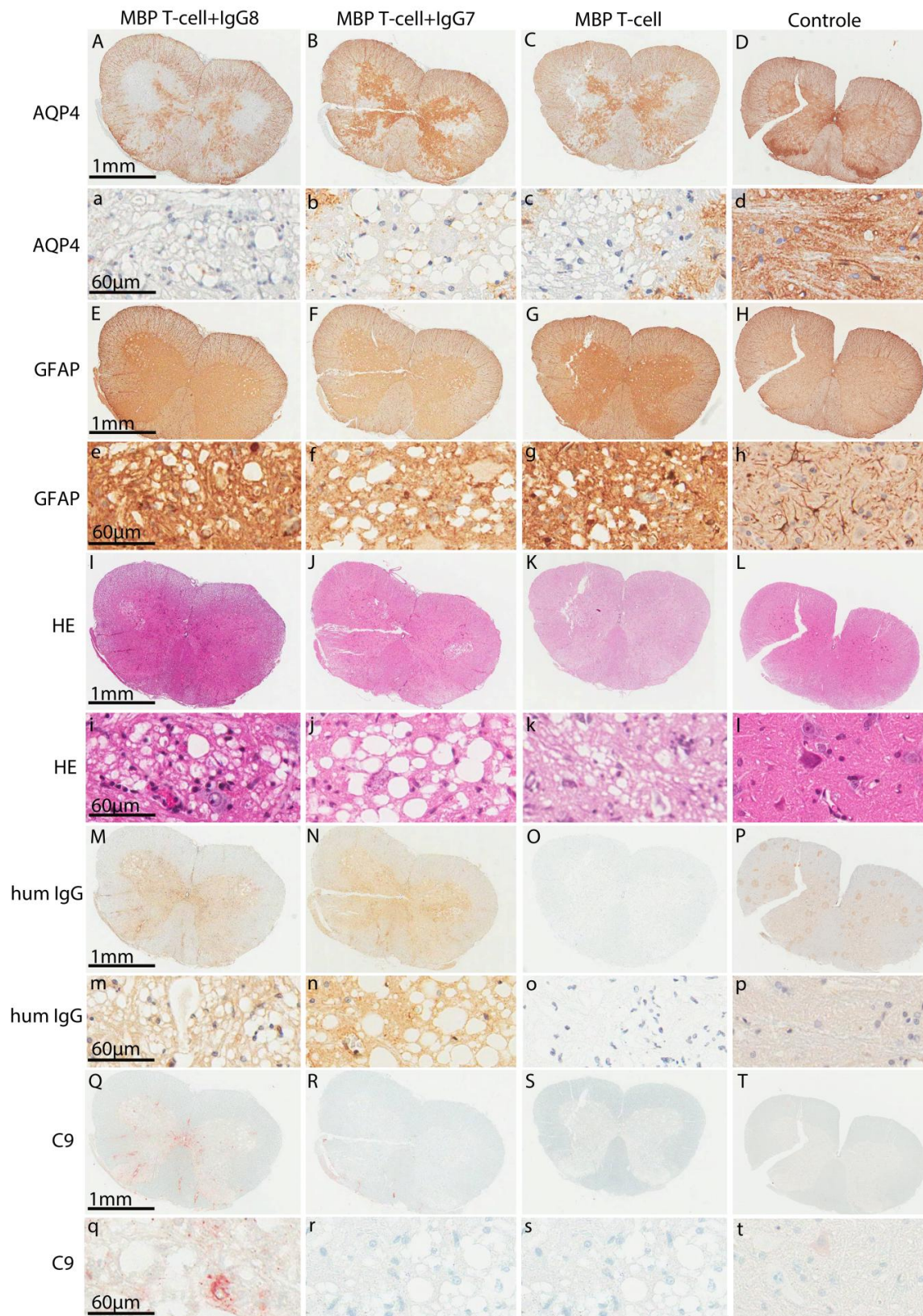


**Figure 19** Representing spinal cord cross sections of animals injected with the 2012 T-cells lines and controls without EAE; examples of vacuolization are displayed from EAE animals treated with and without human NMO IgG for 48h; Profound AQP4 (A-C and a-c) and GFAP (E-G and e-g) loss; Appearing granulocytes (I-K and i-k) compared to control animals (L and l); Human NMO serum (M,N and m,n) and no serum in EAE rat treated with PBS (O and o) and control Lewis rats (P and p); activated compliment but not blood vessel associated (Q and q) or very little complement detection (R, S and r,s).



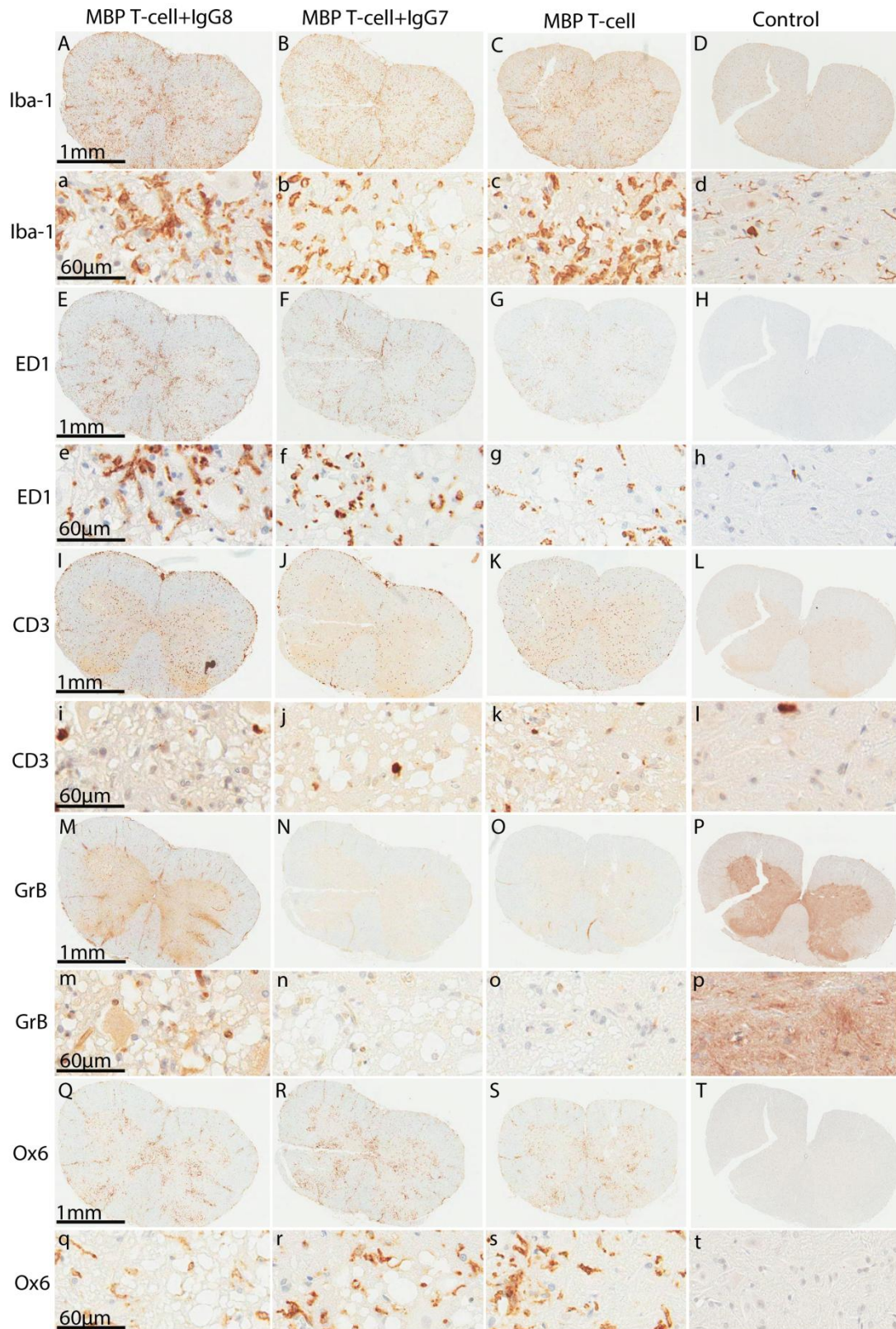


**Figure 20** Representing spinal cord cross sections of animals injected with the 2012 T-cells lines and controls without EAE; examples of vacuolization are displayed from EAE animals treated with and without human NMO IgG for 48h; Strong microglia/macrophage infiltration (A,-C and a-c) and activation (E-G and e-g) compared to controls (D, H and ; Present CD3 positiv T-cells (I-K and i-k) and cytotoxic T-cells (M-O and m-o) in the whole tissue of EAE animals in contrast to controls (L,P and l, p); MHC II expressing cells (Q-S and q-s) in the whole tissue of EAE rats in contrast to controls (T and t)



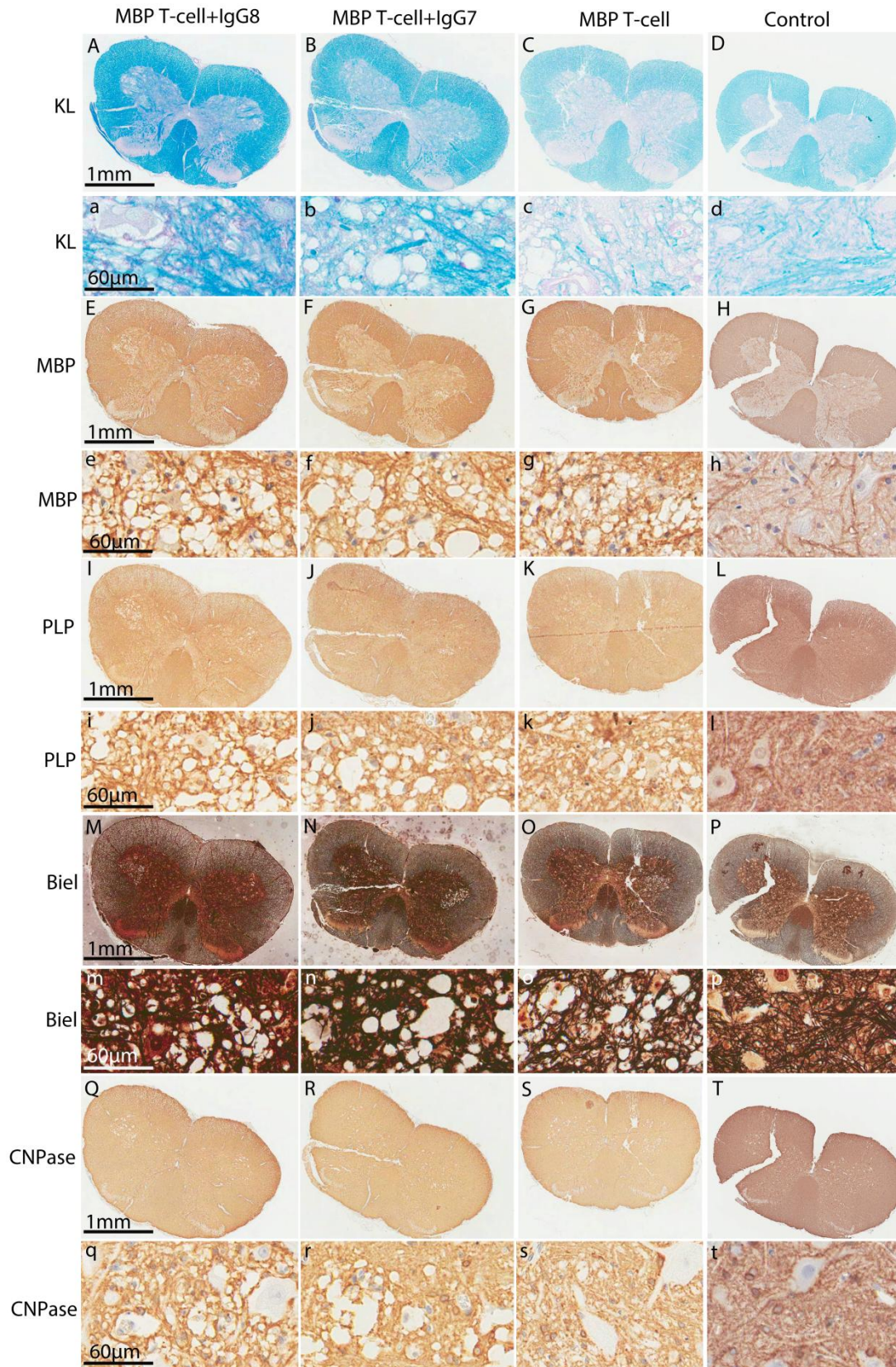


**Figure 21** Representing spinal cord cross sections of animals injected with the 2012 T-cells lines and controls without EAE; examples of vacuolization are displayed from EAE animals treated with and without human NMO IgG for 48h; No myelin loss in Klüver staining could be detected in test group and controls (A-D and a-d); Preserved myelin basic protein (MBP) signal in test groups and controls (E-H and e-h); No myelin proteolipid protein (PLP) loss in EAE rats and controls(I-L and i-l); Intact axons in lesion areas and controls (M-P and m-p); No oligodendrocytic damage in EAE and control animals

**Table 12** Key pathological features in the spinal cord, of EAE induced with different MBP T-cell batches and classical MBP T-cell induced EAE with injection of NMO IgG

	Classical MBP T-cell pathology	Pathology induced by MBP T-cells (MBP7&L-MBP)	Classical MBP T-cell+NMO IgG pathology
AQP4 loss	-	random patchy lesion; +++/++++	Perivascular lesion with sharp lesion edge; +++
GFAP loss	-	random patchy lesion; +++/++++	Perivascular lesion with sharp lesion edge; +++
T-cells	++	+++	+++
Granulocytes	+ / ++	+ / ++	+ / ++
C9	-	-	Perivascular associated
Macrophages / Microglia	+++	+++	+++
Oligodendrocytes loss	-	-	-
Myelin loss	-	-	-
Axon loss	-	-	-

-, minor or absent; +, minor; ++, moderate; +++, severe; +++++, affecting very large areas

## 5.6 No major histocompatibility complex (MHC) II expression on astrocytes in T-cell mediated EAE lesions.

It was shown *in vitro* that astrocytes are capable of major histocompatibility complex (MHC II) expression after treatment with IFN $\gamma$  and that antigen presenting astrocytes can be selectively destroyed by MHC II restricted T-cells in the process of antigen recognition (E Ulvestad, 1994; Fierz et al., 1985; Fontana et al., 1984). It was speculated that such a mechanism could lead to astrocyte loss in T-cell mediated EAE in the absence of pathogenic antibodies.

To investigate this immunofluorescence double staining for astrocytes (GFAP) and MHC II (Ox6) expression was performed using confocal laser microscopy (Figure 22). Profound astrocyte degeneration with very few MHC II expressing microglia in the lesion (Figure 20 A) was seen. In surrounding tissue astrocytes were preserved and intermingled with large numbers of MHC Class II reactive microglia cells (Figure 22 B). However, no cells which showed colocalization of the astrocyte marker GFAP and MHC Class II antigen were present in the tissue.

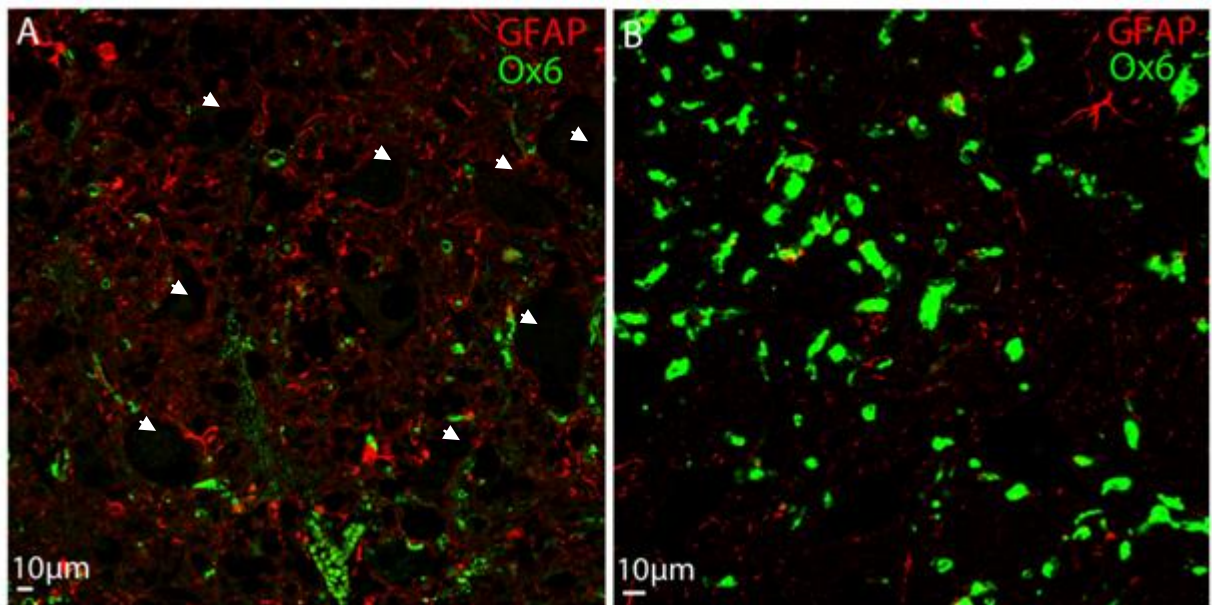


**Figure 22** Representative, Cy2 and Cy3 fluorophor stained, spinal cord cross sections of LM BP7 MBP T-cell line induced EAE animals, with and without human serum containing anti-AQP4 antibody treatment; Lesion with vacuolization (white arrowheads), astrocytic degeneration (red) and little MHC II expressing cells (green). No co-localization of astrocytes and MHC II (A); Preserved astrocytes (red) in neighboring lesion tissue and a profound MHC II expression in other cells (green). No co-localization of astrocytes and MHC II (B)



## 6. Discussion

### 6.1 Cortical lesions

The hypothesis behind the pathological mechanism of NMO is that the anti-AQP4 antibodies can cause complement dependent cytotoxicity (CDC) in the presence of complement (Figure 23 A) and also antibody dependent cellular cytotoxicity (ADCC) when effector cells are present (Figure 23 B) (Hinson et al., 2009; Hinson et al., 2007; Kalluri et al., 2010; Vincent et al., 2008).

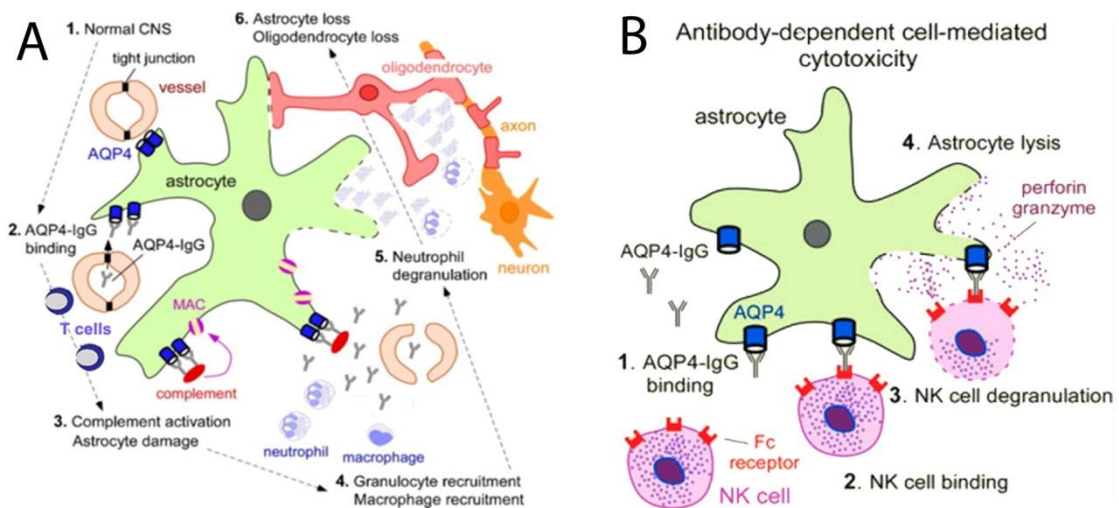


**Figure 23** (A) and (B) NMO pathogenesis mechanism; (A) In the normal CNS, AQP4 is expressed at astrocyte end-feet facing the blood-brain barrier formed by endothelial cells connected by tight junctions (labeled '1'). In NMO, by an unknown mechanism, circulating AQP4-IgG crosses the blood-brain barrier and binds AQP4 on astrocytes (2). This leads to recruitment and activation of complement and deposition of the membrane attack complex (MAC), producing astrocyte damage (3). Complement activation and cytokine secretion by astrocytes recruit inflammatory cells (eosinophils, neutrophils and macrophages), which further disrupt the blood-brain barrier, allowing more entry of AQP4-IgG (4). Degranulating inflammatory cells (5) and astrocyte damage secondarily cause oligodendrocyte injury, myelin loss and axon damage (6); (B) AQP4-IgG binds AQP4 on astrocytes (1). NK cell bind NMO IgG Fc region with the Fc receptor (FcR) (2). The binding induces NK cell degranulation (3) followed by astrocyte lysis (4). Picture and legend are taken and modified from (Ratelade and Verkman, 2012)

The anti-AQP4 antibodies are predominantly of the IgG1 subtype and their Fc region binds complement protein C1q as well as the NK cell receptor FcR (Capel et al., 1994). Recent findings also suggest that NMO IgGs require AQP4 assembly in orthogonal arrays of particles (OAPs), which enhances the binding affinity of the antibodies to AQP4 and further C1q binding to clustered NMO IgG (Phuan et al., 2012).



However, there are several different animal models available to study the pathogenesis of NMO. NMO IgG can be injected in combination with human complement directly into the brain parenchyma of mice (Saadoun et al., 2010). The human complement is necessary, despite the risk of obscuring the action of naturally occurring rodent complement inhibitors, because the mice complement cannot be activated by human IgG. In this model initial AQP4 loss, glial cell edema, minor myelin breakdown and early axonal injury can be observed 12h after injection. After seven days extensive macrophage/microglia and granulocyte infiltration accompanied with perivascular complement depositions, AQP4 and GFAP loss, extensive demyelination and neuronal cell death can be monitored (Saadoun et al., 2010). The advantages of this model are that it requires low concentration of NMO IgG and it suits best for testing of drugs that prevent the binding of the anti-AQP4 antibodies to their cellular targets *in vivo* (Phuan et al., 2012; Tradtrantip et al., 2012) as well as inhibitors of granulocytic effector molecules (Saadoun et al., 2011). The disadvantages are, beside different complement fixation, that it requires surgical manipulations which make it more susceptible to additional inflammatory stimuli in the CNS and that, in relation to mice immune inventory, unphysiological volumes of complement and NMO IgG are injected into the brain (Saadoun et al., 2010). In another model different cytokines are injected into the striatum of NMO IgG seropositive rats to highlight their role in NMO pathology (Kitic et al., 2013). This model shares the same problem of surgical manipulation as the mouse model.

Although intracerebral injection models have some advantages they are not suitable for our purpose. One of the general objectives of our experiments is to find the underlying mechanism of T-cell mediated anti-AQP4 antibody entry through the BBB in NMO, which is not possible with the afore mentioned scientific approaches. Therefore we induced NMO-like lesions by injection of human anti-AQP4 antibodies at the first sign of disease in an experimental autoimmune encephalomyelitis (EAE) rat model (Bennett et al., 2009; Bradl et al., 2009; Kinoshita et al., 2009; Lassmann et al., 1988; Linington et al., 1988). This model is very well established and derives from previous experiences by studying the pathogenicity of antibodies directed against the myelin oligodendrocyte glycoprotein (MOG) (Lassmann et al., 1988; Linington et al., 1988). Thereby MOG antibodies were used after the onset of EAE to induce fixation of complement after binding to the surface of the myelin sheath and initiate demyelination (Lassmann et al., 1988; Linington et al., 1988).

The acute nature of our EAE models enables describing initial tissue alterations seen in the CNS of NMO patients (Bradl et al., 2009). Still, this model also has disadvantages and restrictions. First, NMO lesions in more advanced stages are larger, less specifically directed against astrocytes, show additional demyelination, neuronal and axonal destruction (Lucchinetti et al., 2002) and require a chronic type of model, which was not established yet. Second, the EAE model requires high concentrations of NMO IgG (10 mg) to induce NMO-like pathology. Finally, the inflammation in our EAE model is TH1 driven, whereas in humans there is evidence for additional TH17 influence (Ishizu et al., 2005).

Previously published data could be reproduced in our MBP T-cell induced EAE model, namely that AQP4 antibodies from NMO patients are pathogenic in EAE rats and induce lesions within the spinal cord, which closely reflect those described in the respective human disease (Bradl et al., 2009; Graber et al., 2008; Lucchinetti et al., 2002; Misu et al., 2006; Roemer et al., 2007). The similarities to human NMO lesions are primary loss of AQP4 followed by astrocyte destruction, extensive immunoglobulin and complement deposition on astrocytic foot processes, granulocytic infiltrates, the presence of T-cells and activated microglia/macrophages (Bradl et al., 2009).

One of the goals of my work was to find NMO-like pathology in the cortex of our animal model because there is strong evidence for the mechanisms of NMO causing brain abnormalities in patients (Kim et al., 2011; Li et al., 2008; Saji et al., 2013; Wingerchuk et al., 2006). A recent study (Saji et al., 2013) described AQP4 and GFAP loss in the first cortical layer (C1), but preservation in the underlying layers. Further, inflammation with increased amount of T-cells, B cells and MHC II expressing cells in the meninges and high microglia activity in the second cortical layer (C2) was observed. This inflammatory process was accompanied by significant loss of cortical neurons in C2, C3 and C4.

Interestingly, in most cases the AQP4 and GFAP signal remained preserved in the brains of the NMO IgG treated MBP T-cell induced EAE rats, although strong cortical microglia/macrophage activation and NMO-like lesion formation in the spinal cord of the same animals could be observed. This can have several reasons.

First, encephalitogenic T-cells were present in very low amounts in the meninges surrounding the brain and the cortical parenchyma compared to the spinal cord of the EAE rats. It was shown that NMO IgGs were only pathogenic, when they reach the CNS at sites of brain inflammation (Bradl et al., 2009). It is known that normal Lewis rats which were injected with AQP4 specific antibodies display no NMO-like pathology because under normal conditions the BBB prevents the entry of IgGs into the cerebral spinal fluid (CSF). This makes it unlikely that autoantibody concentrations are reached, which are high enough to initiate lesions (Bradl et al., 2009). The staining for human IgG showed in very few cases that the anti-AQP4 antibodies could reach sufficient amounts in the brain. A possible explanation for this is that in our model, T-cells against myelin basic protein (MBP) induce inflammation mainly in the spinal cord and brain stem, but rarely in other CNS regions possibly making the BBB not permeable for the NMO IgGs in these areas.

Second, not only inflammation and sufficient AQP4 antibody titers are important for NMO-like lesion formation, but also complement binding to the astrocytes associated anti-AQP4 antibodies plays a crucial role in the pathogenicity of NMO (Bradl et al., 2009; Lucchinetti et al., 2002). Depositions of C9 were only present in the cortex after 24h of NMO IgG treatment, but are minor or absent in the EAE animals sacrificed after 72h post IgG injection. In contrast to this, complement deposition signal in the spinal cord could be detected in EAE rats treated with NMO IgG for 24h as well as 72h. This data correlates with the literature where it was described that C9 signal decreases after a few days in the cortex (Merkler et al., 2006) and remains preserved in the spinal cord (Sharma et al., 2010). It is known that, under certain conditions, cells in the CNS are capable of synthesizing all of the complement components (Perry and O'Connor, 2008; Veerhuis et al., 2011; Woodruff et al., 2010). Further it is known that astrocytes have a much higher regulation of complement inhibitor factors than neurons and oligodendrocytes, which only have low levels of complement regulatory factors like decay activating factor (DAF/CD55) and membrane cofactor protein (MCP/CD46). The lack of regulation in these cells makes them more vulnerable to complement associated death than astrocytes (Agoropoulou et al., 1998; Singhrao et al., 2000; Zhang and Verkman, 2014). This also correlates with observations in multiple sclerosis where complement fixation by antibodies, which are restricted to myelin, are found (Genain et al., 1999) and the complement deposition only occurs in the white matter (Brink et al., 2005). The lack of complement in the cortical grey matter also does not

derive from a complete inherited resistance because complement mediated cell damage is found in Rasmussen encephalitis and Alzheimer disease (Eikelenboom and Stam, 1982; Eikelenboom and Veerhuis, 1996; Whitney et al., 1999). With all these findings taken together, it is intriguing to speculate that only low levels of complement fixing antibodies reach the cortex and that moreover complement is depleted due to the upregulation of complement inhibitor proteins in these cells so complement mediated NMO-like lesions cannot form.

Finally, it is possible that initial formation of cortical NMO-like lesions in the targeted EAE may be restricted by accessibility of T-cells and anti-AQP4 antibodies and severity of immune response due to signals from cortical microenvironment e.g. by distinct patterns of chemokine expression (IL-1 $\beta$ ) in the cortex and the spinal cord (Campbell et al., 2002) and followed upregulation of complement production and fixation (Kitic et al., 2013), differences in the T-cell elimination and the permeability of the BBB in various areas of the CNS.

Therefore the use of a different CNS antigen for EAE induction or a different approach for targeting the cortex more specifically on behalf of further analysis of the cortex is suggested. However, the few cortex associated NMO-like lesions displayed very similar pathological features as depicted in the spinal cord of EAE rat model (Bradl et al., 2009) but the described finding in the cortex of NMO patients (Saji et al., 2013) could not be reproduced.

## **6.2 T-cell induced astrocyte damage**

Two specific MBP T-cell lines induced lesions with AQP4 and GFAP loss in the spinal cord of EAE animals. In contrast to NMO IgG related lesions these lesions were not located around vessels, did not contain a sharp lesion edge towards the unaffected CNS tissue, but rather appeared diffuse and displayed profound tissue vacuolization (spongy degeneration). The presence of AQP4 and GFAP loss could be due to MBP presentation by MHC II expressing astrocytes to T-cells, as it has been shown *in vitro* (E Ulvestad, 1994; Fierz et al., 1985; Fontana et al., 1984), and that these antigen presenting astroglia could be selectively destroyed by MHC II restricted CD4<sup>+</sup> T-cells. As already described, no evidence for MHC Class II protein expression on astrocytes could be found. This does, however, not exclude that very

low MHC Class II expression on astrocytes, which escapes immunocytochemical detection, may be sufficient for antigen presentation and activation of CD4+ T-cells.

In addition, other mechanisms alone or in combination could lead to astrocyte damage. One study showed that activated CD4+ T-cells can induce tissue injuries in an antigen presentation independent way during the migration into the CNS parenchyma (Nitsch et al., 2004). Thereby receptor mediated glutamate toxicity and direct damage by cytotoxic granules may lead to calcium overload and cell death (Choi, 1995; Nicotera and Orrenius, 1998; Yu et al., 2001)

Another study showed that local injection of lipopolysaccharide (LPS) in the spinal cord can induce AQP4 loss with astrocyte degeneration (Sharma et al., 2010). The underlying mechanism is unknown, but it has been suggested that LPS activated microglia/macrophages produce a large amounts of proinflammatory molecules like TNF $\alpha$ , IL-1 $\beta$  or nitric oxide (NO), which have been shown to impair astrocytic function *in vitro* (Retamal et al., 2007).

It was also shown that astrocytes play an important role in modulating the innate-to-adaptive immune response. They express a variety of receptors linked to innate immune system such as mannose receptors, scavenger receptors, toll-like receptors (TLRs), nucleotide binding oligomerization domains and dsRNA dependent protein kinases (Farina et al., 2007). Activated astroglia produce cytokines like IL-1, IL-6, IL-10, IL-33 and TNF- $\alpha$  and chemokines e.g. MCP-1, IL-8, CCL-5 and IP-10 (Carpentier et al., 2005; Chakraborty et al., 2010; Oh et al., 1999).

Finally, IL-1 $\beta$  production leads to accumulation of complement, induces the breakdown of the BBB and enables the entry of granulocytes (Kitic et al., 2013).

The mechanism behind the T-cell induced astrocytic pathology is still unclear. Additional phenotyping regarding chemokine and cytokine expression of this particular T-cell line is required, but all the findings mentioned above indicate that lesion formation with loss of AQP4 and GFAP can occur in inflammatory lesions of the CNS independent from NMO IgG. Thus, experimental studies aimed to investigate the potential role of CNS specific antibodies *in vitro* and *in vivo* have to be based on proper control experiments, which exclude non-specific immune mediated tissue injury.

## 7. Conclusion

I demonstrated that different NMO IgGs differ in their ability to induce microglia/macrophage activation in T-cell mediated inflammatory environment and that microglia activation increases with time after onset of inflammation and antibody exposure.

I was unable to reproduce the NMO specific cortical pathology described by Saji et al. in NMO patients, although NMO-like lesions can be induced in principle in the cortex of rats with autoimmune encephalomyelitis in the presence of NMO-IgG.

Finally I found that astrocyte destructive lesions can be also induced by CD4+ T-cells directed against the myelin antigen myelin basic protein.

## 8. Acknowledgements

First of all I would like to thank Prof. Dr. Lassmann for giving me the opportunity to work in his lab on my master-thesis. He was very patient with me and helped me with his comments and ideas through this thesis, and I am very thankful for that. Especially I want to thank Marianne Leißer, Ulrike Köck and Angela Kury, I am very grateful for all the technical assistance. Without them I still would search for antibodies in the fridge. Further I want to thank Assoc. Prof. Dr. Monika Bradl for providing me with valuable information on my topic. I want to thank Prof. Jan Bauer for the help concerning the confocal-microscope and with his immunohistochemical expertise.

Furthermore I want to thank my colleagues: Cornelia Schuh, Simon Hametner, Isabella Wimmer, Niko Kögl, Satoru Ogi, Taro Kadowaki, Antonia Rudel, and Joana Santos for very interesting and inspiring talks and new ideas.

My special gratitude belongs to Maja Kitic, Maria Pohl, Bleranda Zeka, Tobias Zrzavy and Lukas Haider, who have also supported me during practical work and thereby saved me a lot of time in the laboratory.

Most of all I want to thank my parents Tomislav and Marina, my sister and correction hero Nika and the rest of my family and friends, who have always supported me and helped me to manage my degree.

## 9. References

- Aboul-Enein, F., Bauer, J., Klein, M., Schubart, A., Flugel, A., Ritter, T., Kawakami, N., Siedler, F., Linington, C., Wekerle, H., *et al.* (2004). Selective and antigen-dependent effects of myelin degeneration on central nervous system inflammation. *J Neuropathol Exp Neurol* 63, 1284-1296.
- Agoropoulou, C., Piddlesden, S.J., Lachmann, P.J., and Wing, M.G. (1998). Neuronal protection of oligodendrocytes from antibody-independent complement lysis. *Neuroreport* 9, 927-932.
- Apiwattanakul, M., Popescu, B.F., Matiello, M., Weinshenker, B.G., Lucchinetti, C.F., Lennon, V.A., McKeon, A., Carpenter, A.F., Miller, G.M., and Pittock, S.J. (2010). Intractable vomiting as the initial presentation of neuromyelitis optica. *Ann Neurol* 68, 757-761.
- Asgari, N., Owens, T., Frøkjaer, J., Stenager, E., Lillevang, S.T., and Kyvik, K.O. (2011b). Neuromyelitis optica (NMO) - an autoimmune disease of the central nervous system (CNS). *Acta Neurologica Scandinavica* 123, 369-384.
- Ben-Nun, A., Wekerle, H., and Cohen, I.R. (1981). The rapid isolation of clonable antigen-specific T lymphocyte lines capable of mediating autoimmune encephalomyelitis. *Eur J Immunol* 11, 195-199.
- Bennett, J.L., Lam, C., Kalluri, S.R., Saikali, P., Bautista, K., Dupree, C., Glogowska, M., Case, D., Antel, J.P., Owens, G.P., *et al.* (2009). Intrathecal pathogenic anti-aquaporin-4 antibodies in early neuromyelitis optica. *Annals of Neurology* 66, 617-629.
- Bourre, B., Marignier, R., Zephir, H., Papeix, C., Brassat, D., Castelnovo, G., Collongues, N., Vukusic, S., Labauge, P., Outteryck, O., *et al.* (2012). Neuromyelitis optica and pregnancy. *Neurology* 78, 875-879.
- Bradl, M., Misu, T., Takahashi, T., Watanabe, M., Mader, S., Reindl, M., Adzemovic, M., Bauer, J., Berger, T., Fujihara, K., *et al.* (2009). Neuromyelitis optica: Pathogenicity of patient immunoglobulin in vivo. *Annals of Neurology* 66, 630-643.
- Brink, B.P., Veerhuis, R., Breij, E.C., van der Valk, P., Dijkstra, C.D., and Bo, L. (2005). The pathology of multiple sclerosis is location-dependent: no significant complement activation is detected in purely cortical lesions. *J Neuropathol Exp Neurol* 64, 147-155.
- Calabrese, M., Oh, M.S., Favaretto, A., Rinaldi, F., Poretto, V., Alessio, S., Lee, B.C., Yu, K.H., Ma, H.I., Perini, P., *et al.* (2012). No MRI evidence of cortical lesions in neuromyelitis optica. *Neurology* 79, 1671-1676.
- Campbell, S.J., Wilcockson, D.C., Butchart, A.G., Perry, V.H., and Anthony, D.C. (2002). Altered chemokine expression in the spinal cord and brain contributes to differential interleukin-1beta-induced neutrophil recruitment. *J Neurochem* 83, 432-441.



Capel, P.J., van de Winkel, J.G., van den Herik-Oudijk, I.E., and Verbeek, J.S. (1994). Heterogeneity of human IgG Fc receptors. *Immunomethods* 4, 25-34.

Carpentier, P.A., Begolka, W.S., Olson, J.K., Elhofy, A., Karpus, W.J., and Miller, S.D. (2005). Differential activation of astrocytes by innate and adaptive immune stimuli. *Glia* 49, 360-374.

Chakraborty, S., Kaushik, D.K., Gupta, M., and Basu, A. (2010). Inflammasome signaling at the heart of central nervous system pathology. *J Neurosci Res* 88, 1615-1631.

Choi, D.W. (1995). Calcium: still center-stage in hypoxic-ischemic neuronal death. *Trends Neurosci* 18, 58-60.

Cornelio, D.B., Braga, R.P., Rosa, M.W., and Ayub, A.C. (2009). Devic's neuromyelitis optica and pregnancy: distinction from multiple sclerosis is essential. *Arch Gynecol Obstet* 280, 475-477.

Cree, B.A., Lamb, S., Morgan, K., Chen, A., Waubant, E., and Genain, C. (2005). An open label study of the effects of rituximab in neuromyelitis optica. *Neurology* 64, 1270-1272.

Davis, R., Thiele, E., Barnes, P., and Riviello, J.J., Jr. (1996). Neuromyelitis optica in childhood: case report with sequential MRI findings. *J Child Neurol* 11, 164-167.

E Ulvestad, K.W., L Bø, B Trapp, J Antel, and S Mørk (1994). HLA class II molecules (HLA-DR, -DP, -DQ) on cells in the human CNS studied in situ and in vitro. *Immunology* 82(4): 535–541.

Eikelenboom, P., and Stam, F.C. (1982). Immunoglobulins and complement factors in senile plaques. An immunoperoxidase study. *Acta Neuropathol* 57, 239-242.

Eikelenboom, P., and Veerhuis, R. (1996). The role of complement and activated microglia in the pathogenesis of Alzheimer's disease. *Neurobiol Aging* 17, 673-680.

Esiri, M.M. (1980). Multiple sclerosis: a quantitative and qualitative study of immunoglobulin-containing cells in the central nervous system. *Neuropathol Appl Neurobiol* 6, 9-21.

Esiri, M.M., Reading, M.C., Squier, M.V., and Hughes, J.T. (1989). Immunocytochemical characterization of the macrophage and lymphocyte infiltrate in the brain in six cases of human encephalitis of varied aetiology. *Neuropathol Appl Neurobiol* 15, 289-305.

Farina, C., Aloisi, F., and Meinl, E. (2007). Astrocytes are active players in cerebral innate immunity. *Trends Immunol* 28, 138-145.

Fierz, W., Endler, B., Reske, K., Wekerle, H., and Fontana, A. (1985). Astrocytes as antigen-presenting cells. I. Induction of Ia antigen expression on astrocytes by T cells via immune interferon and its effect on antigen presentation. *J Immunol* 134, 3785-3793.

Filippi, M., Rocca, M.A., Moiola, L., Martinelli, V., Ghezzi, A., Capra, R., Salvi, F., and Comi, G. (1999). MRI and magnetization transfer imaging changes in the brain and cervical cord of patients with Devic's neuromyelitis optica. *Neurology* 53, 1705-1710.

Fontana, A., Fierz, W., and Wekerle, H. (1984). Astrocytes present myelin basic protein to encephalitogenic T-cell lines. *Nature* 307, 273-276.

Fujihara, K., Misu, T., Nakashima, I., Takahashi, T., Bradl, M., Lassmann, H., Takano, R., Nishiyama, S., Takai, Y., Suzuki, C., *et al.* (2012). Neuromyelitis optica should be classified as an astrocytopathic disease rather than a demyelinating disease. *Clinical and Experimental Neuroimmunology* 3, 58-73.

Genain, C.P., Cannella, B., Hauser, S.L., and Raine, C.S. (1999). Identification of autoantibodies associated with myelin damage in multiple sclerosis. *Nat Med* 5, 170-175.

Gold, R., Linington, C., and Lassmann, H. (2006). Understanding pathogenesis and therapy of multiple sclerosis via animal models: 70 years of merits and culprits in experimental autoimmune encephalomyelitis research. *Brain* 129, 1953-1971.

Graber, D.J., Levy, M., Kerr, D., and Wade, W.F. (2008). Neuromyelitis optica pathogenesis and aquaporin 4. *Journal of Neuroinflammation* 5, 22.

Hinson, S.R., McKeon, A., Fryer, J.P., Apiwattanakul, M., Lennon, V.A., and Pittock, S.J. (2009). Prediction of neuromyelitis optica attack severity by quantitation of complement-mediated injury to aquaporin-4-expressing cells. *Arch Neurol* 66, 1164-1167.

Hinson, S.R., Pittock, S.J., Lucchinetti, C.F., Roemer, S.F., Fryer, J.P., Kryzer, T.J., and Lennon, V.A. (2007). Pathogenic potential of IgG binding to water channel extracellular domain in neuromyelitis optica. *Neurology* 69, 2221-2231.

Ishizu, T., Osoegawa, M., Mei, F.J., Kikuchi, H., Tanaka, M., Takakura, Y., Minohara, M., Murai, H., Mihara, F., Taniwaki, T., *et al.* (2005). Intrathecal activation of the IL-17/IL-8 axis in optico-spinal multiple sclerosis. *Brain* 128, 988-1002.

Jarius, S., Aboul-Enein, F., Waters, P., Kuenz, B., Hauser, A., Berger, T., Lang, W., Reindl, M., Vincent, A., and Kristoferitsch, W. (2008a). Antibody to aquaporin-4 in the long-term course of neuromyelitis optica. *Brain* 131, 3072-3080.

Jarius, S., Paul, F., Franciotta, D., Waters, P., Zipp, F., Hohlfeld, R., Vincent, A., and Wildemann, B. (2008). Mechanisms of disease: aquaporin-4 antibodies in neuromyelitis optica. *Nat Clin Pract Neurol* 4, 202-214.

Jarius, S., and Wildemann, B. (2010). AQP4 antibodies in neuromyelitis optica: diagnostic and pathogenetic relevance. *Nature Reviews Neurology* 6, 383-392.

Kalluri, S.R., Illes, Z., Srivastava, R., Cree, B., Menge, T., Bennett, J.L., Berthele, A., and Hemmer, B. (2010). Quantification and functional characterization of antibodies to native aquaporin 4 in neuromyelitis optica. *Arch Neurol* 67, 1201-1208.

Kim, J.E., Kim, S.M., Ahn, S.W., Lim, B.C., Chae, J.H., Hong, Y.H., Park, K.S., Sung, J.J., and Lee, K.W. (2011). Brain abnormalities in neuromyelitis optica. *J Neurol Sci* 302, 43-48.

Kim, W., Kim, S.H., Lee, S.H., Li, X.F., and Kim, H.J. (2011b). Brain abnormalities as an initial manifestation of neuromyelitis optica spectrum disorder. *Mult Scler* 17, 1107-1112.

Kim, W., Park, M.S., Lee, S.H., Kim, S.H., Jung, I.J., Takahashi, T., Misu, T., Fujihara, K., and Kim, H.J. (2010). Characteristic brain magnetic resonance imaging abnormalities in central nervous system aquaporin-4 autoimmunity. *Mult Scler* 16, 1229-1236.

Kinoshita, M., Nakatsuji, Y., Kimura, T., Moriya, M., Takata, K., Okuno, T., Kumanogoh, A., Kajiya, K., Yoshikawa, H., and Sakoda, S. (2009). Neuromyelitis optica: Passive transfer to rats by human immunoglobulin. *Biochem Biophys Res Commun* 386, 623-627.

Kitic, M., Hochmeister, S., Wimmer, I., Bauer, J., Misu, T., Mader, S., Reindl, M., Fujihara, K., Lassmann, H., and Bradl, M. (2013). Intrastriatal injection of interleukin-1 beta triggers the formation of neuromyelitis optica-like lesions in NMO-IgG seropositive rats. *Acta Neuropathol Commun* 1, 5.

Kobayashi, Z., Tsuchiya, K., Uchihara, T., Nakamura, A., Haga, C., Yokota, O., Ishizu, H., Taki, K., Arai, T., Akiyama, H., *et al.* (2009). Intractable hiccup caused by medulla oblongata lesions: a study of an autopsy patient with possible neuromyelitis optica. *J Neurol Sci* 285, 241-245.

Lassmann, H. (2005). Multiple sclerosis pathology: evolution of pathogenetic concepts. *Brain Pathol* 15, 217-222.

Lassmann, H., Brunner, C., Bradl, M., and Linington, C. (1988). Experimental allergic encephalomyelitis: the balance between encephalitogenic T lymphocytes and demyelinating antibodies determines size and structure of demyelinated lesions. *Acta Neuropathol* 75, 566-576.

Lennon, V., Wingerchuk, D., Kryzer, T., Pittock, S., Lucchinetti, C., Fujihara, K., Nakashima, I., and Weinshenker, B. (2004). A serum autoantibody marker of neuromyelitis optica: distinction from multiple sclerosis. *The Lancet* 364, 2106-2112.

Lennon, V.A. (2005). IgG marker of optic-spinal multiple sclerosis binds to the aquaporin-4 water channel. *Journal of Experimental Medicine* 202, 473-477.

Li, Y., Xie, P., Lv, F., Mu, J., Li, Q., Yang, Q., Hu, M., Tang, H., and Yi, J. (2008). Brain magnetic resonance imaging abnormalities in neuromyelitis optica. *Acta Neurol Scand* 118, 218-225.

Linington, C., Berger, T., Perry, L., Weerth, S., Hinze-Selch, D., Zhang, Y., Lu, H.C., Lassmann, H., and Wekerle, H. (1993). T cells specific for the myelin oligodendrocyte glycoprotein mediate an unusual autoimmune inflammatory response in the central nervous system. *Eur J Immunol* 23, 1364-1372.

Linington, C., Bradl, M., Lassmann, H., Brunner, C., and Vass, K. (1988). Augmentation of demyelination in rat acute allergic encephalomyelitis by circulating mouse monoclonal antibodies directed against a myelin/oligodendrocyte glycoprotein. *Am J Pathol* 130, 443-454.

Lucchinetti, C.F., Mandler, R.N., McGavern, D., Bruck, W., Gleich, G., Ransohoff, R.M., Trebst, C., Weinshenker, B., Wingerchuk, D., Parisi, J.E., *et al.* (2002). A role for humoral mechanisms in the pathogenesis of Devic's neuromyelitis optica. *Brain* 125, 1450-1461.

Matiello, M., Lennon, V.A., Jacob, A., Pittock, S.J., Lucchinetti, C.F., Wingerchuk, D.M., and Weinshenker, B.G. (2008). NMO-IgG predicts the outcome of recurrent optic neuritis. *Neurology* 70, 2197-2200.

Merkler, D., Ernsting, T., Kerschensteiner, M., Bruck, W., and Stadelmann, C. (2006). A new focal EAE model of cortical demyelination: multiple sclerosis-like lesions with rapid resolution of inflammation and extensive remyelination. *Brain* 129, 1972-1983.

Misu, T., Fujihara, K., Kakita, A., Konno, H., Nakamura, M., Watanabe, S., Takahashi, T., Nakashima, I., Takahashi, H., and Itoyama, Y. (2007). Loss of aquaporin 4 in lesions of neuromyelitis optica: distinction from multiple sclerosis. *Brain* 130, 1224-1234.

Misu, T., Fujihara, K., Nakamura, M., Murakami, K., Endo, M., Konno, H., and Itoyama, Y. (2006). Loss of aquaporin-4 in active perivascular lesions in neuromyelitis optica: a case report. *Tohoku J Exp Med* 209, 269-275.

Misu, T., Fujihara, K., Nakashima, I., Sato, S., and Itoyama, Y. (2005). Intractable hiccup and nausea with periaqueductal lesions in neuromyelitis optica. *Neurology* 65, 1479-1482.

Misu, T., Höftberger, R., Fujihara, K., Wimmer, I., Takai, Y., Nishiyama, S., Nakashima, I., Konno, H., Bradl, M., Garzuly, F., *et al.* (2013). Presence of six different lesion types suggests diverse mechanisms of tissue injury in neuromyelitis optica. *Acta Neuropathologica*.

Mokhtarian, F., McFarlin, D.E., and Raine, C.S. (1984). Adoptive transfer of myelin basic protein-sensitized T cells produces chronic relapsing demyelinating disease in mice. *Nature* 309, 356-358.

Morris-Downes, M.M., Smith, P.A., Rundle, J.L., Piddlesden, S.J., Baker, D., Pham-Dinh, D., Heijmans, N., and Amor, S. (2002). Pathological and regulatory effects of anti-myelin antibodies in experimental allergic encephalomyelitis in mice. *J Neuroimmunol* 125, 114-124.

Nakamura, M., Miyazawa, I., Fujihara, K., Nakashima, I., Misu, T., Watanabe, S., Takahashi, T., and Itoyama, Y. (2008). Preferential spinal central gray matter involvement in neuromyelitis optica. An MRI study. *J Neurol* 255, 163-170.

Nandhagopal, R., Al-Asmi, A., and Gujjar, A.R. (2010). Neuromyelitis optica: an overview. *Postgrad Med J* 86, 153-159.

Nicotera, P., and Orrenius, S. (1998). The role of calcium in apoptosis. *Cell Calcium* 23, 173-180.

Nishiyama, S., Ito, T., Misu, T., Takahashi, T., Kikuchi, A., Suzuki, N., Jin, K., Aoki, M., Fujihara, K., and Itoyama, Y. (2009). A case of NMO seropositive for aquaporin-4 antibody more than 10 years before onset. *Neurology* 72, 1960-1961.

Nitsch, R., Pohl, E.E., Smorodchenko, A., Infante-Duarte, C., Aktas, O., and Zipp, F. (2004). Direct impact of T cells on neurons revealed by two-photon microscopy in living brain tissue. *J Neurosci* 24, 2458-2464.

Oh, J.W., Schwiebert, L.M., and Benveniste, E.N. (1999). Cytokine regulation of CC and CXC chemokine expression by human astrocytes. *J Neurovirol* 5, 82-94.

Parratt, J.D., and Prineas, J.W. (2010). Neuromyelitis optica: a demyelinating disease characterized by acute destruction and regeneration of perivascular astrocytes. *Mult Scler* 16, 1156-1172.

Perry, V.H., and O'Connor, V. (2008). C1q: the perfect complement for a synaptic feast? *Nat Rev Neurosci* 9, 807-811.

Petzold, A., Marignier, R., Verbeek, M.M., and Confavreux, C. (2011). Glial but not axonal protein biomarkers as a new supportive diagnostic criteria for Devic neuromyelitis optica? Preliminary results on 188 patients with different neurological diseases. *J Neurol Neurosurg Psychiatry* 82, 467-469.

Phuan, P.W., Anderson, M.O., Tradtrantip, L., Zhang, H., Tan, J., Lam, C., Bennett, J.L., and Verkman, A.S. (2012). A Small-molecule Screen Yields Idiotypic-specific Blockers of Neuromyelitis Optica Immunoglobulin G Binding to Aquaporin-4. *Journal of Biological Chemistry* 287, 36837-36844.

Phuan, P.W., Ratelade, J., Rossi, A., Tradtrantip, L., and Verkman, A.S. (2012b). Complement-dependent cytotoxicity in neuromyelitis optica requires aquaporin-4 assembly in orthogonal arrays. *Journal of Biological Chemistry*.

Pittock, S., Weinshenker, B.G., Lucchinetti, C.F., Wingerchuk, D.M., Corboy, J.R., and Lennon, V.A. (2006). Neuromyelitis optica brain lesions localized at sites of high aquaporin 4 expression. *Archives of Neurology* 63, 964-968.

Pittock, S.J., Lennon, V.A., Krecke, K., Wingerchuk, D.M., Lucchinetti, C.F., and Weinshenker, B.G. (2006). Brain abnormalities in neuromyelitis optica. *Arch Neurol* 63, 390-396.

Popescu, B.F., Lennon, V.A., Parisi, J.E., Howe, C.L., Weigand, S.D., Cabrera-Gomez, J.A., Newell, K., Mandler, R.N., Pittock, S.J., Weinshenker, B.G., *et al.* (2011). Neuromyelitis optica unique area postrema lesions: nausea, vomiting, and pathogenic implications. *Neurology* 76, 1229-1237.

Popescu, B.F., Parisi, J.E., Cabrera-Gomez, J.A., Newell, K., Mandler, R.N., Pittock, S.J., Lennon, V.A., Weinshenker, B.G., and Lucchinetti, C.F. (2010). Absence of cortical demyelination in neuromyelitis optica. *Neurology* 75, 2103-2109.

Ransohoff, R.M. (2012). Illuminating neuromyelitis optica pathogenesis. *Proceedings of the National Academy of Sciences* 109, 1001-1002.

Ratelade, J., and Verkman, A.S. (2012). Neuromyelitis optica: aquaporin-4 based pathogenesis mechanisms and new therapies. *Int J Biochem Cell Biol* 44, 1519-1530.

Retamal, M.A., Froger, N., Palacios-Prado, N., Ezan, P., Saez, P.J., Saez, J.C., and Giaume, C. (2007). Cx43 hemichannels and gap junction channels in astrocytes are regulated oppositely by proinflammatory cytokines released from activated microglia. *J Neurosci* 27, 13781-13792.

Rocca, M.A., Agosta, F., Mezzapesa, D.M., Martinelli, V., Salvi, F., Ghezzi, A., Bergamaschi, R., Comi, G., and Filippi, M. (2004). Magnetization transfer and diffusion tensor MRI show gray matter damage in neuromyelitis optica. *Neurology* 62, 476-478.

Roemer, S.F., Parisi, J.E., Lennon, V.A., Benarroch, E.E., Lassmann, H., Bruck, W., Mandler, R.N., Weinshenker, B.G., Pittock, S.J., Wingerchuk, D.M., *et al.* (2007). Pattern-specific loss of aquaporin-4 immunoreactivity distinguishes neuromyelitis optica from multiple sclerosis. *Brain* 130, 1194-1205.

Saadoun, S., Waters, P., Bell, B.A., Vincent, A., Verkman, A.S., and Papadopoulos, M.C. (2010). Intra-cerebral injection of neuromyelitis optica immunoglobulin G and human complement produces neuromyelitis optica lesions in mice. *Brain* 133, 349-361.

Saadoun, S., Waters, P., MacDonald, C., Bridges, L.R., Bell, B.A., Vincent, A., Verkman, A.S., and Papadopoulos, M.C. (2011). T cell deficiency does not reduce lesions in mice produced by intracerebral injection of NMO-IgG and complement. *Journal of Neuroimmunology* 235, 27-32.

Saiki, S., Ueno, Y., Moritani, T., Sato, T., Sekine, T., Kawajiri, S., Adachi, S., Yokoyama, K., Tomizawa, Y., Motoi, Y., *et al.* (2009). Extensive hemispheric lesions with radiological evidence of blood-brain barrier integrity in a patient with neuromyelitis optica. *J Neurol Sci* 284, 217-219.

Saji, E., Arakawa, M., Yanagawa, K., Toyoshima, Y., Yokoseki, A., Okamoto, K., Otsuki, M., Akazawa, K., Kakita, A., Takahashi, H., *et al.* (2013). Cognitive impairment and cortical degeneration in neuromyelitis optica. *Ann Neurol* 73, 65-76.

Sato, D., and Fujihara, K. (2011). Atypical presentations of neuromyelitis optica. *Arq Neuropsiquiatr* 69, 824-828.

Sharma, R., Fischer, M.-T., Bauer, J., Felts, P.A., Smith, K.J., Misu, T., Fujihara, K., Bradl, M., and Lassmann, H. (2010). Inflammation induced by innate immunity in the central nervous system leads to primary astrocyte dysfunction followed by demyelination. *Acta Neuropathologica* 120, 223-236.

Singhrao, S.K., Neal, J.W., Rushmere, N.K., Morgan, B.P., and Gasque, P. (2000). Spontaneous classical pathway activation and deficiency of membrane regulators render human neurons susceptible to complement lysis. *Am J Pathol* 157, 905-918.

Suzuki, N., Takahashi, T., Aoki, M., Misu, T., Konohana, S., Okumura, T., Takahashi, H., Kameya, S., Yamaki, K., Kumagai, T., *et al.* (2010). Neuromyelitis optica preceded by hyperCKemia episode. *Neurology* 74, 1543-1545.

Takahashi, T., Fujihara, K., Nakashima, I., Misu, T., Miyazawa, I., Nakamura, M., Watanabe, S., Shiga, Y., Kanaoka, C., Fujimori, J., *et al.* (2007). Anti-aquaporin-4 antibody is involved in the pathogenesis of NMO: a study on antibody titre. *Brain* 130, 1235-1243.

Takahashi, T., Miyazawa, I., Misu, T., Takano, R., Nakashima, I., Fujihara, K., Tobita, M., and Itoyama, Y. (2008). Intractable hiccup and nausea in neuromyelitis optica with anti-aquaporin-4 antibody: a herald of acute exacerbations. *J Neurol Neurosurg Psychiatry* 79, 1075-1078.

Tanaka, M., Matsushita, T., Tateishi, T., Ochi, H., Kawano, Y., Mei, F.J., Minohara, M., Murai, H., and Kira, J.I. (2008). Distinct CSF cytokine/chemokine profiles in atopic myelitis and other causes of myelitis. *Neurology* 71, 974-981.

Tradtrantip, L., Zhang, H., Saadoun, S., Phuan, P.W., Lam, C., Papadopoulos, M.C., Bennett, J.L., and Verkman, A.S. (2012). Anti-aquaporin-4 monoclonal antibody blocker therapy for neuromyelitis optica. *Ann Neurol* 71, 314-322.

Traugott, U., Reinherz, E.L., and Raine, C.S. (1983). Multiple sclerosis. Distribution of T cells, T cell subsets and Ia-positive macrophages in lesions of different ages. *J Neuroimmunol* 4, 201-221.

Tsugawa, J., Tsuboi, Y., Inoue, H., Baba, Y., and Yamada, T. (2010). [A case of anti-aquaporin 4 antibody-positive Sjogren syndrome associated with a relapsed myelitis in pregnancy]. *Rinsho Shinkeigaku* 50, 27-30.

Vaknin-Dembinsky, A., Brill, L., Kassis, I., Petrou, P., Ovadia, H., Ben-Hur, T., Abramsky, O., and Karussis, D. (2012). T-cell reactivity against AQP4 in neuromyelitis optica. *Neurology* 79, 945-946.

Veerhuis, R., Nielsen, H.M., and Tenner, A.J. (2011). Complement in the brain. *Mol Immunol* 48, 1592-1603.

Vincent, T., Saikali, P., Cayrol, R., Roth, A.D., Bar-Or, A., Prat, A., and Antel, J.P. (2008). Functional consequences of neuromyelitis optica-IgG astrocyte interactions on blood-brain barrier permeability and granulocyte recruitment. *J Immunol* 181, 5730-5737.

Wang, K.C., Lee, C.L., Chen, S.Y., Chen, J.C., Yang, C.W., Chen, S.J., and Tsai, C.P. (2013). Distinct serum cytokine profiles in neuromyelitis optica and multiple sclerosis. *J Interferon Cytokine Res* 33, 58-64.

Waters, P., Jarius, S., Littleton, E., Leite, M.I., Jacob, S., Gray, B., Ghera, R., Vale, T., Jacob, A., Palace, J., *et al.* (2008). Aquaporin-4 antibodies in neuromyelitis optica and longitudinally extensive transverse myelitis. *Arch Neurol* 65, 913-919.

Whitney, K.D., Andrews, P.I., and McNamara, J.O. (1999). Immunoglobulin G and complement immunoreactivity in the cerebral cortex of patients with Rasmussen's encephalitis. *Neurology* 53, 699-708.

Wingerchuk, D.M., Hogancamp, W.F., O'Brien, P.C., and Weinshenker, B.G. (1999). The clinical course of neuromyelitis optica (Devic's syndrome). *Neurology* 53, 1107-1114.

Wingerchuk, D.M., Lennon, V.A., Lucchinetti, C.F., Pittock, S.J., and Weinshenker, B.G. (2007). The spectrum of neuromyelitis optica. *The Lancet Neurology* 6, 805-815.

Wingerchuk, D.M., Lennon, V.A., Pittock, S.J., Lucchinetti, C.F., and Weinshenker, B.G. (2006). Revised diagnostic criteria for neuromyelitis optica. *Neurology* 66, 1485-1489.

Wingerchuk, D.M., Pittock, S.J., Lucchinetti, C.F., Lennon, V.A., and Weinshenker, B.G. (2007). A secondary progressive clinical course is uncommon in neuromyelitis optica. *Neurology* 68, 603-605.

Woodruff, T.M., Ager, R.R., Tenner, A.J., Noakes, P.G., and Taylor, S.M. (2010). The role of the complement system and the activation fragment C5a in the central nervous system. *Neuromolecular Med* 12, 179-192.

Yu, C., Lin, F., Li, K., Jiang, T., Qin, W., Sun, H., and Chan, P. (2008). Pathogenesis of normal-appearing white matter damage in neuromyelitis optica: diffusion-tensor MR imaging. *Radiology* 246, 222-228.

Yu, C.S., Lin, F.C., Li, K.C., Jiang, T.Z., Zhu, C.Z., Qin, W., Sun, H., and Chan, P. (2006). Diffusion tensor imaging in the assessment of normal-appearing brain tissue damage in relapsing neuromyelitis optica. *AJNR Am J Neuroradiol* 27, 1009-1015.

Yu, S.P., Canzoniero, L.M., and Choi, D.W. (2001). Ion homeostasis and apoptosis. *Curr Opin Cell Biol* 13, 405-411.

Zhang, H., and Verkman, A.S. (2014). Longitudinally extensive NMO spinal cord pathology produced by passive transfer of NMO-IgG in mice lacking complement inhibitor CD59. *J Autoimmun.*



# Curriculum vitae

## Education

---

- 2011-2014** Master in Molecular Biology (with main focus on Neuroscience) and Master in Immunology and Microbiology (with main focus on Immunology)
- 2013-2014** Work for second masterthesis at the CBR (Center for Brain research) at the Department for Bioelectronics  
Uni Wien, Austria; Expected date of graduation June 2014
- 2012-2014** Work for masterthesis at the CBR (Center for Brain research) at the department for Neuroimmunology  
Uni Wien, Austria.
- 2007-2011** Bachelor in Genetic and Microbiology at the MFPL (Max F. Perutz Laboratories)  
Uni Wien, Austria.
- 2007** Military service in the Austrian Armed Forces  
"4. Gardekompanie", Austria
- 1998-2006** Highschool  
"Bundesgymnasium und Bundesrealgymnasium Zirkusgasse", Austria

## Further education and internships

---

**July 2012 PADI** (Professional Association of Diving Instructors) Divemaster certification (allows guiding people under water and assisting diving instructors during courses).

**Aug.-Sep. 2011** Two months internship in Baxter Innovations GmbH, Orth an der Donau, Austria. Subject: Cellular Processing under Good Laboratory Practice (GLP) conditions in a stage three safety laboratory

**Jan. 2011** Bioinformatics course, at the IMP (Institute of Molecular Pathology)

**Sep. 2010** Internship in Baxter Innovations GmbH, Orth an der Donau, Austria. Subject: Cellular Processing under Good Laboratory Practice (GLP) conditions in a stage three safety laboratory

**Oct. 2010** Practical course: Molecular analysis of gene expression, at the Cancer Research Institute, Medical University of Vienna.

**Mar. 2010** Practical course: Bioverfahrenstechnik, at the TU Wien (Technical University)

Oral presentation

---

**1<sup>st</sup> CLARITY USERS Meeting, 7<sup>th</sup> April 2014**

London, United Kingdom. Immunohistochemistry and 3D reconstruction of clarified tissue.